

Black-Box Certification with Randomized Smoothing: A Functional Optimization Based Framework

Dinghuai Zhang^{*1} Mao Ye^{*2} Chengyue Gong^{*2} Zhanxing Zhu¹ Qiang Liu²

Abstract

Randomized classifiers have been shown to provide a promising approach for achieving certified robustness against adversarial attacks in deep learning. However, most existing methods only leverage Gaussian smoothing noise and only work for ℓ_2 perturbation. We propose a general framework of adversarial certification with non-Gaussian noise and for more general types of attacks, from a unified functional optimization perspective. Our new framework allows us to identify a key trade-off between accuracy and robustness via designing smoothing distributions, helping to design new families of non-Gaussian smoothing distributions that work more efficiently for different ℓ_p settings, including ℓ_1 , ℓ_2 and ℓ_∞ attacks. Our proposed methods achieve better certification results than previous works and provide a new perspective on randomized smoothing certification.

1. Introduction

Deep neural networks have achieved state-of-the-art performance on many tasks such as image classification (He et al., 2016) and language modeling (Devlin et al., 2019). Nonetheless, modern deep learning models are highly sensitive to small and adversarially crafted perturbations on the inputs (Goodfellow et al., 2015), which means that human-imperceptible changes on inputs could cause the model to make dramatically different predictions. Although many robust training algorithms have been developed to overcome adversarial attacking, most heuristically developed methods can be shown to be broken by more powerful adversaries eventually, (e.g., Athalye et al., 2018; Madry et al., 2018; Zhang et al., 2019; Wang et al., 2019). This casts an urgent demand for developing robust classifiers with provable worst-case guarantees.

One promising approach for certifiable robustness is the recent *randomized smoothing method* (Lecuyer et al., 2018; Cohen et al., 2019; Salman et al., 2019; Lee et al., 2019; Li et al., 2019; Dvijotham et al., 2020; Teng et al., 2020; Jia et al., 2020), which constructs smoothed classifiers with certifiable robustness by introducing noise on the inputs. Compared with the other more traditional certification approaches (Wong & Kolter, 2017; Dvijotham et al., 2018; Jordan et al., 2019) that exploits special structures of the neural networks (such as the properties of ReLU), the randomized smoothing methods work more flexibly on general black-box classifiers and is shown to be more scalable and provide tighter bounds on challenging datasets such as ImageNet (Deng et al., 2009).

In addition, most existing randomized smoothing methods use Gaussian noise for smoothing. Although appearing to be a natural choice, one of our key observations is that the Gaussian distribution is, in fact, a sub-optimal choice in high dimensional spaces, even for ℓ_2 attack. Our observation shows there is a counter-intuitive phenomenon in high dimensional spaces (Vershynin, 2018), that almost all of the probability mass of standard Gaussian distribution concentrates around the sphere surface of a certain radius. This makes tuning the variance of Gaussian distribution an inefficient way to trade off robustness and accuracy for randomized smoothing.

Our Contributions We propose a general framework of adversarial certification using non-Gaussian smoothing noises, based on a new functional optimization perspective. Our framework unifies the methods of Cohen et al. (2019) and Teng et al. (2020) as special cases, and is applicable to more general smoothing distributions and more types of attacks beyond ℓ_2 -norm setting. Leveraging our insight, we develop a new family of distributions for better certification results on ℓ_1 , ℓ_2 and ℓ_∞ attacks. An efficient computational approach is developed to enable our method in practice. Empirical results show that our new framework and smoothing distributions outperform existing approaches for ℓ_1 , ℓ_2 and ℓ_∞ attacking, on datasets such as CIFAR-10 and ImageNet.

^{*}Equal contribution ¹Peking University, Beijing, China
²University of Texas at Austin, Austin, USA. Correspondence to: Dinghuai Zhang <zhangdinghuai@pku.edu.cn>.

2. Related Works

Empirical Defenses Since Szegedy et al. (2013) and Goodfellow et al. (2015), many previous works have focused on utilizing small perturbation δ under certain constraint, e.g. in a ℓ_p norm ball, to attack a neural network. Adversarial training (Madry et al., 2018) and its variants (Kannan et al., 2018; Zhang & Wang, 2019; Zhai et al., 2019) are the most successful defense methods. However, these empirical defense methods are still easy to be broken and cannot provide provable defenses.

Certified Defenses Unlike the empirical defense methods, once a classifier can guarantee a consistent prediction for input within a local region, it is called a certified-robustness classifier. *Exact* certification methods provide the minimal perturbation condition which leads to a different classification result. This line of work focus on deep neural networks with ReLU-like activation that makes the classifier a piecewise linear function. This enables researchers to introduce satisfiability modulo theories (Carlini et al., 2017; Ehlers, 2017) or mix integer linear programming (Cheng et al., 2017; Dutta et al., 2018). *Sufficient* certification methods take a conservative way and bound the Lipschitz constant or other information of the network (Jordan et al., 2019; Wong & Kolter, 2017; Raghunathan et al., 2018; Zhang et al., 2018). However, these certification strategies share a drawback that they are not feasible on large-scale scenarios, e.g. large and deep networks and datasets.

Randomized Smoothing To mitigate this limitation of previous certifiable defenses, improving network robustness via randomness has been recently discussed (Xie et al., 2018; Liu et al., 2018). Lecuyer et al. (2018) first introduced randomization with technique in differential privacy. Li et al. (2019) improved their work with a bound given by Rényi divergence. In succession, Cohen et al. (2019) firstly provided a *tight* bound for *arbitrary* Gaussian smoothed classifiers based on previous theorems found by Li & Kuelbs (1998). Salman et al. (2019) combined the empirical and certification robustness, by applying adversarial training on randomized smoothed classifiers to achieve a higher certified accuracy. Lee et al. (2019) focused on ℓ_0 norm perturbation setting, and proposed a discrete smoothing distribution which can be shown perform better than the widely used Gaussian distribution. Teng et al. (2020) took a similar statistical testing approach with Cohen et al. (2019), utilizing Laplacian smoothing to tackle ℓ_1 certification problem. Jia et al. (2020) extended the approach of Cohen et al. (2019) to a top-k setting. Dvijotham et al. (2020) extends the total variant used by Cohen et al. (2019) to f -divergences. We also focus on a generalization of randomized smoothing, but with a different view on loosening the constrain about classifier.

3. Black-box Certification with Functional Optimization

We start from introducing background of the adversarial certification problem and the randomized smoothing method. In Section 3.2, we propose our general framework for adversarial certification using general smoothing noises, from a new functional optimization perspective. Our framework unifies the method of Cohen et al. (2019); Teng et al. (2020) as special cases, and reveals a potential trade-off between accuracy and robustness that provides important guidance for better choices of smoothing distributions in Section 4.

3.1. Background

Adversarial Certification For simplicity, we consider binary classification of predicting binary labels $y \in \{0, 1\}$ given feature vectors $x \in \mathbb{R}^d$. The extension to multi-class cases is straightforward, and is discussed in Appendix D. Furthermore, we assume $f^\sharp: \mathbb{R}^d \rightarrow [0, 1]$ is a given binary classifier (\sharp means the classifier is *given*), which maps from the input space \mathbb{R}^d to either the positive class probability in interval $[0, 1]$ or binary labels in $\{0, 1\}$. In the robustness certification problem, a testing data point $x_0 \in \mathbb{R}^d$ is given, and one is asked to verify if the classifier outputs the same prediction when the input x_0 is perturbed arbitrarily in \mathcal{B} , a given neighborhood of x_0 . Specifically, let \mathcal{B} be a set of possible perturbation vectors, e.g., $\mathcal{B} = \{\delta \in \mathbb{R}^d : \|\delta\|_p \leq r\}$ for ℓ_p norm with a radius r . If the classifier predicts $y = 1$ on x_0 , i.e. $f^\sharp(x_0) > 1/2$, we want to verify if $f^\sharp(x_0 + \delta) > 1/2$ still holds for any $\delta \in \mathcal{B}$. Through this paper, we consider the most common adversarial settings: ℓ_1 , ℓ_2 and ℓ_∞ attacks.

Black-box Randomized Smoothing Certification Directly certifying f^\sharp heavily relies on the smooth property of f^\sharp , which has been explored in a series of prior works (Wong & Kolter, 2017; Lecuyer et al., 2018). These methods typically depend on the special structure-property (e.g., the use of ReLU units) of f^\sharp , and thus can not serve as general-purpose algorithms for any type of networks. Instead, We are interested in *black-box* verification methods that could work for *arbitrary* classifiers. One approach to enable this, as explored in recent works (Cohen et al., 2019; Lee et al., 2019), is to replace f^\sharp with a smoothed classifier by convolving it with Gaussian noise, and verify the *smoothed* classifier.

Specifically, assume π_0 is a smoothing distribution with zero mean and bounded variance, e.g., $\pi_0 = \mathcal{N}(\mathbf{0}, \sigma^2)$. The randomized smoothed classifier is defined by

$$f_{\pi_0}^\sharp(x_0) := \mathbb{E}_{z \sim \pi_0} [f^\sharp(x_0 + z)],$$

which returns the averaged probability of $x_0 + z$ under the perturbation of $z \sim \pi_0$. Assume we replace the original

classifier with $f_{\pi_0}^\sharp$, then the goal becomes certifying $f_{\pi_0}^\sharp$ using its inherent smoothness. Specifically, if $f_{\pi_0}^\sharp(\mathbf{x}_0) > 1/2$, we want to certify that $f_{\pi_0}^\sharp(\mathbf{x}_0 + \delta) > 1/2$ for every $\delta \in \mathcal{B}$, that is, we want to certify that

$$\min_{\delta \in \mathcal{B}} f_{\pi_0}^\sharp(\mathbf{x}_0 + \delta) = \min_{\delta \in \mathcal{B}} \mathbb{E}_{z \sim \pi_0} [f^\sharp(\mathbf{x}_0 + z + \delta)] > \frac{1}{2}. \quad (1)$$

In this case, it is sufficient to obtain a *guaranteed lower bound* of $\min_{\delta \in \mathcal{B}} f_{\pi_0}^\sharp(\mathbf{x}_0 + \delta)$ and check if it is larger than $1/2$. When π_0 is Gaussian $\mathcal{N}(\mathbf{0}, \sigma^2)$ and for ℓ_2 attack, this problem was studied in [Cohen et al. \(2019\)](#), which shows that a lower bound of

$$\min_{z \in \mathcal{B}} \mathbb{E}_{z \sim \pi_0} [f^\sharp(\mathbf{x}_0 + z)] \geq \Phi(\Phi^{-1}(f_{\pi_0}^\sharp(\mathbf{x}_0)) - \frac{r}{\sigma}), \quad (2)$$

where $\Phi(\cdot)$ is the cumulative density function (CDF) of standard Gaussian distribution, and $\Phi^{-1}(\cdot)$ represents its inverse cumulative distribution function. The proof of this result in [Cohen et al. \(2019\)](#) uses Neyman-Pearson lemma ([Li & Kuelbs, 1998](#)). In the following section, we will show that this bound is a special case of the proposed functional optimization framework for robustness certification.

Note that the bound in Equation (2) is tractable since it only requires to evaluate the smoothed classifier $f_{\pi_0}^\sharp(\mathbf{x}_0)$ at the original image \mathbf{x}_0 , instead of solving the difficult adversarial optimization over perturbation z in Equation (1). In practice, $f_{\pi_0}^\sharp(\mathbf{x}_0)$ is approximated by Monte Carlo approximation with a non-asymptotic confidence bound.

3.2. Constrained Adversarial Certification

We propose a **constrained adversarial certification (CAC)** framework, which yields a guaranteed lower bound for Equation (1). The main idea is simple: assume \mathcal{F} is a function class which is known to include f^\sharp , then the following optimization immediately yields a guaranteed lower bound

$$\min_{\delta \in \mathcal{B}} f_{\pi_0}^\sharp(\mathbf{x}_0 + \delta) \geq \min_{f \in \mathcal{F}} \min_{\delta \in \mathcal{B}} \left\{ f_{\pi_0}(\mathbf{x}_0 + \delta) \text{ s.t. } f_{\pi_0}(\mathbf{x}_0) = f_{\pi_0}^\sharp(\mathbf{x}_0) \right\}, \quad (3)$$

where we define $f_{\pi_0}(\mathbf{x}_0) = \mathbb{E}_{z \sim \pi_0} [f(\mathbf{x}_0 + z)]$ for any given f . Then we need to search for the minimum value of $f_{\pi_0}(\mathbf{x}_0 + \delta)$ for all classifiers in \mathcal{F} that satisfies $f_{\pi_0}(\mathbf{x}_0) = f_{\pi_0}^\sharp(\mathbf{x}_0)$. This obviously yields a lower bound once $f^\sharp \in \mathcal{F}$. If \mathcal{F} includes only f^\sharp , then the bound is exact, but is computationally prohibitive due to the difficulty of optimizing δ . The idea is then to choose \mathcal{F} properly to incorporate rich information of f^\sharp , while allowing us to calculate the lower bound in Equation (3) computationally tractably. In this paper, we consider the set of all functions bounded in $[0, 1]$,

namely

$$\mathcal{F}_{[0,1]} = \left\{ f : f(z) \in [0, 1], \forall z \in \mathbb{R}^d \right\}, \quad (4)$$

which guarantees to include all f^\sharp by definition. There are other \mathcal{F} that also yields computationally tractable bounds, including the L_p functional space $\mathcal{F} = \{f : \|f\|_{L_p} \leq v\}$, which we leave for future work.

Denote by $\mathcal{L}_{\pi_0}(\mathcal{F}, \mathcal{B})$ the lower bound in Equation (3). We can rewrite it into the following minimax form using the Lagrangian function,

$$\begin{aligned} \mathcal{L}_{\pi_0}(\mathcal{F}, \mathcal{B}) &= \min_{f \in \mathcal{F}} \min_{\delta \in \mathcal{B}} \max_{\lambda \in \mathbb{R}} L(f, \delta, \lambda) \\ &\triangleq \min_{f \in \mathcal{F}} \min_{\delta \in \mathcal{B}} \max_{\lambda \in \mathbb{R}} \left\{ f_{\pi_0}(\mathbf{x}_0 + \delta) - \lambda(f_{\pi_0}(\mathbf{x}_0) - f_{\pi_0}^\sharp(\mathbf{x}_0)) \right\}, \end{aligned} \quad (5)$$

where λ is the Lagrangian multiplier. Exchanging the min and max yields the following dual form.

Theorem 1. I) (Dual Form) Denote by π_δ the distribution of $z + \delta$ when $z \sim \pi_0$. Assume \mathcal{F} and \mathcal{B} are compact set. We have the following lower bound of $\mathcal{L}_{\pi_0}(\mathcal{F}, \mathcal{B})$:

$$\begin{aligned} \mathcal{L}_{\pi_0}(\mathcal{F}, \mathcal{B}) &\geq \max_{\lambda \geq 0} \min_{f \in \mathcal{F}} \min_{\delta \in \mathcal{B}} L(f, \delta, \lambda) \\ &= \max_{\lambda \geq 0} \left\{ \lambda f_{\pi_0}^\sharp(\mathbf{x}_0) - \max_{\delta \in \mathcal{B}} \mathbb{D}_{\mathcal{F}}(\lambda \pi_0 \parallel \pi_\delta) \right\}, \end{aligned} \quad (6)$$

where we define the discrepancy term $\mathbb{D}_{\mathcal{F}}(\lambda \pi_0 \parallel \pi_\delta)$ as

$$\max_{f \in \mathcal{F}} \left\{ \lambda \mathbb{E}_{z \sim \pi_0} [f(\mathbf{x}_0 + z)] - \mathbb{E}_{z \sim \pi_\delta} [f(\mathbf{x}_0 + z)] \right\},$$

which measures the difference of $\lambda \pi_0$ and π_δ by seeking the maximum discrepancy of the expectation for $f \in \mathcal{F}$. As we will show later, the bound in (6) is computationally tractable with proper $(\mathcal{F}, \mathcal{B}, \pi_0)$.

II) When $\mathcal{F} = \mathcal{F}_{[0,1]} := \{f : f(x) \in [0, 1], x \in \mathbb{R}^d\}$, we have in particular

$$\mathbb{D}_{\mathcal{F}_{[0,1]}}(\lambda \pi_0 \parallel \pi_\delta) = \int (\lambda \pi_0(z) - \pi_\delta(z))_+ dz,$$

where $(t)_+ = \max(0, t)$. Furthermore, we have $0 \leq \mathbb{D}_{\mathcal{F}_{[0,1]}}(\lambda \pi_0 \parallel \pi_\delta) \leq \lambda$ for any π_0, π_δ and $\lambda > 0$. Note that $\mathbb{D}_{\mathcal{F}_{[0,1]}}(\lambda \pi_0 \parallel \pi_\delta)$ coincides with the total variation distance between π_0 and π_δ when $\lambda = 1$.

III) (Strong duality) Suppose $\mathcal{F} = \mathcal{F}_{[0,1]}$ and suppose that for any $\lambda \geq 0$, $\min_{\delta \in \mathcal{B}} \min_{f \in \mathcal{F}_{[0,1]}} L(f, \delta, \lambda) = \min_{f \in \mathcal{F}_{[0,1]}} L(f, \delta^*, \lambda)$, for some $\delta^* \in \mathcal{B}$, we have

$$V_{\pi_0}(\mathcal{F}, \mathcal{B}) = \max_{\lambda \geq 0} \min_{\delta \in \mathcal{B}} \min_{f \in \mathcal{F}} L(f, \delta, \lambda).$$

Remark We will show later that the proposed methods and the cases we study satisfy the condition in part III of the theorem and thus all the lower bounds of the proposed method are tight.

Proof. First, observe that the constraint in Equation (3) can be equivalently replaced by an inequality constraint $f_{\pi_0}(\mathbf{x}_0) \geq f_{\pi_0}^\#(\mathbf{x}_0)$. Therefore, the Lagrangian multiplier can be restricted to be $\lambda \geq 0$. We have

$$\begin{aligned} \mathcal{L}_{\pi_0}(\mathcal{F}, \mathcal{B}) &= \min_{\delta \in \mathcal{B}} \min_{f \in \mathcal{F}} \max_{\lambda \geq 0} \mathbb{E}_{\pi_\delta}[f(\mathbf{x}_0 + \mathbf{z})] \\ &\quad + \lambda (f_{\pi_0}^\#(\mathbf{x}_0) - \mathbb{E}_{\pi_0}[f(\mathbf{x}_0 + \mathbf{z})]) \\ &\geq \max_{\lambda \geq 0} \min_{\delta \in \mathcal{B}} \min_{f \in \mathcal{F}} \mathbb{E}_{\pi_\delta}[f(\mathbf{x}_0 + \mathbf{z})] \\ &\quad + \lambda (f_{\pi_0}^\#(\mathbf{x}_0) - \mathbb{E}_{\pi_0}[f(\mathbf{x}_0 + \mathbf{z})]) \\ &= \max_{\lambda \geq 0} \min_{\delta \in \mathcal{B}} \left\{ \lambda f_{\pi_0}^\#(\mathbf{x}_0) \right. \\ &\quad \left. + \min_{f \in \mathcal{F}} \mathbb{E}_{\pi_\delta}[f(\mathbf{x}_0 + \mathbf{z})] - \lambda \mathbb{E}_{\pi_0}[f(\mathbf{x}_0 + \mathbf{z})] \right\} \\ &= \max_{\lambda \geq 0} \min_{\delta \in \mathcal{B}} \{ \lambda f_{\pi_0}^\#(\mathbf{x}_0) - \mathbb{D}_{\mathcal{F}}(\lambda \pi_0 \parallel \pi_\delta) \} \end{aligned}$$

The proof of the strong duality is in Appendix A.1. II) follows a straightforward calculation. \square

Although the lower bound in Equation (6) still involves an optimization on δ and λ , both of them are much easier than the original adversarial optimization in Equation (1). With proper choices of \mathcal{F} , \mathcal{B} and π_0 , the optimization of δ can be shown to provide simple closed-form solutions by exploiting the symmetry of \mathcal{B} , and the optimization of λ is a very simple one-dimensional searching problem.

As corollaries of Theorem 1, we can exactly recover the bound derived by Teng et al. (2020) and Cohen et al. (2019) under our functional optimization framework, different from their original Neyman-Pearson lemma approach.

Corollary 1. *With Laplacian noise $\pi_0(\cdot) = \text{Laplace}(\cdot; b)$, where $\text{Laplace}(\mathbf{x}; b) = \frac{1}{(2b)^d} \exp(-\frac{\|\mathbf{x}\|_1}{b})$, ℓ_1 adversarial setting $\mathcal{B} = \{\delta: \|\delta\|_1 \leq r\}$ and $\mathcal{F} = \mathcal{F}_{[0,1]}$, the lower bound in Equation (6) becomes*

$$\begin{aligned} \max_{\lambda \geq 0} \left\{ \lambda f_{\pi_0}^\#(\mathbf{x}_0) - \max_{\|\delta\|_1 \leq r} \mathbb{D}_{\mathcal{F}_{[0,1]}}(\lambda \pi_0 \parallel \pi_\delta) \right\} &= \\ \begin{cases} 1 - e^{r/b}(1 - f_{\pi_0}^\#(\mathbf{x}_0)), & \text{when } f_{\pi_0}^\#(\mathbf{x}_0) \geq 1 - \frac{1}{2}e^{-r/b} \\ \frac{1}{2}e^{-\frac{r}{b} - \log[2(1 - f_{\pi_0}^\#(\mathbf{x}_0))]}, & \text{when } f_{\pi_0}^\#(\mathbf{x}_0) < 1 - \frac{1}{2}e^{-r/b} \end{cases} \end{aligned} \quad (7)$$

Thus, with our previous explanation,

$$\mathcal{L}_{\pi_0}(\mathcal{F}, \mathcal{B}) \geq \frac{1}{2} \iff r \leq -b \log[2(1 - f_{\pi_0}^\#(\mathbf{x}_0))],$$

which is exactly the ℓ_1 certification radius derived by Teng et al. (2020). See Appendix A.2 for proof details.

For Gaussian noise setting which has been frequently adopted, we have

Corollary 2. *With isotropic Gaussian noise $\pi_0 = \mathcal{N}(\mathbf{0}, \sigma^2 I_{d \times d})$, ℓ_2 attack $\mathcal{B} = \{\delta: \|\delta\|_2 \leq r\}$ and $\mathcal{F} = \mathcal{F}_{[0,1]}$, the lower bound in Equation (6) becomes*

$$\begin{aligned} \max_{\lambda \geq 0} \left\{ \lambda f_{\pi_0}^\#(\mathbf{x}_0) - \max_{\|\delta\|_2 \leq r} \mathbb{D}_{\mathcal{F}_{[0,1]}}(\lambda \pi_0 \parallel \pi_\delta) \right\} \\ = \Phi \left(\Phi^{-1}(f_{\pi_0}^\#(\mathbf{x}_0)) - \frac{r}{\sigma} \right). \end{aligned} \quad (8)$$

Analogously, we can retrieve the main theoretical result of Cohen et al. (2019):

$$\mathcal{L}_{\pi_0}(\mathcal{F}, \mathcal{B}) \geq \frac{1}{2} \iff r \leq \sigma \Phi^{-1}(f_{\pi_0}^\#(\mathbf{x}_0)).$$

See Appendix A.3 for proof details.

3.3. Trade-off between Accuracy and Robustness

The lower bound in Equation (6) reflects an intuitive trade-off between the robustness and accuracy on the certification problem:

$$\max_{\lambda \geq 0} \left[\underbrace{\lambda f_{\pi_0}^\#(\mathbf{x}_0)}_{\text{Accuracy}} - \underbrace{\max_{\delta \in \mathcal{B}} \mathbb{D}_{\mathcal{F}}(\lambda \pi_0 \parallel \pi_\delta)}_{\text{Robustness}} \right], \quad (9)$$

where the first term reflects the accuracy of the smoothed classifier (assuming the true label is $y = 1$), while the second term $\max_{\delta \in \mathcal{B}} \mathbb{D}_{\mathcal{F}}(\lambda \pi_0 \parallel \pi_\delta)$ measures the robustness of the smoothing method, via the maximum difference between the original smoothing distribution π_0 and perturbed distribution π_δ for $\delta \in \mathcal{B}$. The maximization of dual coefficient λ can be viewed as searching for a best balance between these two terms to achieve the largest lower bound.

More critically, different choices of smoothing distributions also yield a trade-off between accuracy and robustness in Equation (9). A good choice of the smoothing distribution should well balance the accuracy and robustness, by distributing its mass properly to yield small $\max_{\delta \in \mathcal{B}} \mathbb{D}_{\mathcal{F}}(\lambda \pi_0 \parallel \pi_\delta)$ and large $f_{\pi_0}^\#(\mathbf{x}_0)$ simultaneously.

4. Improving Certification Bounds with a New Distribution Family

In this section, we identify a key problem of the usage of Laplacian and Gaussian noise in high dimensional space,

due to the “thin shell” phenomenon that the probability mass of them concentrates on a sphere far away from the center points (Vershynin, 2018). Motivated by this pivotal observation, we propose a new family of smoothing distributions that alleviate this problem for ℓ_1 , ℓ_2 and ℓ_∞ attack.

4.1. A New Distribution Family

Although the isotropic Gaussian distribution appears to be a natural choice of the smoothing distribution, they are sub-optimal for a trade-off between accuracy and robustness in Equation (9), especially in high dimensions. The key problem is that, in high dimensional spaces, the probability mass of Gaussian distributions concentrates on a *thin shell* away from the center. Specifically,

Lemma 1 (Vershynin (2018), Section 3.1). *Let $z \sim \mathcal{N}(\mathbf{0}, I_{d \times d})$ be a d -dimensional standard Gaussian random variable. Then there exists a constant c , such that for any $\delta \in (0, 1)$, $\text{Prob}(\sqrt{d} - \sqrt{c \log(2/\delta)} \leq \|z\|_2 \leq \sqrt{d} + \sqrt{c \log(2/\delta)}) \geq 1 - \delta$. See Vershynin (2018) for more discussion.*

This suggests that with high probability, z takes values very close to the sphere of radius \sqrt{d} , within a constant distance from that sphere. There exists similar phenomenon for Laplacian distribution:

Lemma 2 (Chebyshev bound). *Let z be a d -dimensional Laplacian random variable, $z = (z_1, \dots, z_d)$, where $z_i \sim \text{Laplace}(1)$, $i = 1, \dots, d$. Then for any $\delta \in (0, 1)$, we have $\text{Prob}(1 - 1/\sqrt{d\delta} \leq \|z\|_1/d \leq 1 + 1/\sqrt{d\delta}) \geq 1 - \delta$.*

This phenomenon makes it sub-optimal to use standard Gaussian or Laplacian distribution for adversarial certification, because one would expect that the smoothing distribution should concentrate around the center (the original image) in order to make the smoothed classifier close to the original classifier (and hence accurate). To illustrate the problem, consider a simple example when the true classifier is $f^\sharp(x) = \mathbb{I}(\|x - x_0\|_2 \leq \epsilon\sqrt{d})$ for a constant $\epsilon < 1$, where \mathbb{I} is the indicator function. Then when the dimension d is large, we would have $f^\sharp(x_0) = 1$ while $f_{\pi_0}^\sharp(x_0) \approx 0$ when $\pi_0 = \mathcal{N}(\mathbf{0}, I_{d \times d})$. It is of course possible to decrease the variance of π_0 to improve the accuracy of the smoothed classifier $f_{\pi_0}^\sharp$. However, this would significantly improve the distance term in Equation (9) and does not yield an optimal trade-off on accuracy and robustness.

In this work, we introduce a new distribution family to address this curse of dimensionality. To motivate our method, it is useful to examine the density function of the distributions of the radius of spherical distributions in general.

Lemma 3. *Assume z is a symmetric random variable on \mathbb{R}^d with a probability density function (PDF) of form $\pi_0(z) \propto \phi(\|z\|)$, where $\phi: [0, \infty) \rightarrow [0, \infty)$ is a univariate function,*

then the PDF of the norm of z is $p_{\|z\|}(r) \propto r^{d-1}\phi(r)$. The term r^{d-1} arises due to the integration on the surface of radius r norm ball in \mathbb{R}^d . Here $\|\cdot\|$ can be any L_p norm.

In particular, when $z \sim \mathcal{N}(\mathbf{0}, \sigma^2 I_{d \times d})$, we have $\phi(r) = \exp(-r^2/(2\sigma^2))$ and hence $p_{\|z\|_2}(r) \propto r^{d-1} \exp(-r^2/(2\sigma^2))$, which is a scaled Chi distribution, also known as *Nakagami distribution*. Examining this PDF, we can see that the concentration of the norm is caused by the r^{d-1} term, which makes the density to be highly peaked when d is large. To alleviate the concentration phenomenon, we need to have a way to cancel out the effect of r^{d-1} . This motivates the following family of smoothing distributions:

$$\pi_0(z) \propto \|z\|_{n_1}^{-k} \exp\left(-\frac{\|z\|_{n_2}^p}{b}\right),$$

where parameters $n_1, n_2, p \in \mathbb{N}$. How to choose suitable n_1 and n_2 is depend on the perturbation region.

4.2. ℓ_1 and ℓ_2 Region Certification

We propose typical distribution belongs to the proposed distribution family for ℓ_1 and ℓ_2 region certification.

For the ℓ_2 case, we propose:

$$\pi_0(z) \propto \|z\|_2^{-k} \exp\left(-\frac{\|z\|_2^2}{2\sigma^2}\right), \quad (10)$$

$$\text{and hence } p_{\|z\|_2}(r) \propto r^{d-k-1} \exp\left(-\frac{r^2}{2\sigma^2}\right),$$

where we introduce the $\|z\|_2^{-k}$ term in π_0 , with k a positive parameter, to make the radius distribution less concentrated when k is large. As for ℓ_1 certification, we also introduce a $\|z\|_1^{-k}$ term to force a more centralized distribution:

$$\pi_0(z) \propto \|z\|_1^{-k} \exp\left(-\frac{\|z\|_1}{b}\right), \quad (11)$$

$$\text{and hence } p_{\|z\|_1}(r) \propto r^{d-k-1} \exp\left(-\frac{r}{b}\right).$$

The radius distribution in Equation (10) and Equation (11) is controlled by two parameters: σ (or b) and k , where σ (or b) controls the scale of the distribution (and is hence the *scale parameter*), while k controls the shape of the distribution (and hence the *shape parameter*). The key idea is that adjusting k allows us to control the trade-off the accuracy and robustness more precisely. As shown in Figure 1, adjusting σ enables us to move the mean close to zero (hence yielding higher accuracy), but at cost of decreasing the variance quadratically (hence less robust). In contrast, adjusting k allows us to decrease the mean without significantly impacting the variance, and hence yield a much better trade-off on accuracy and robustness.

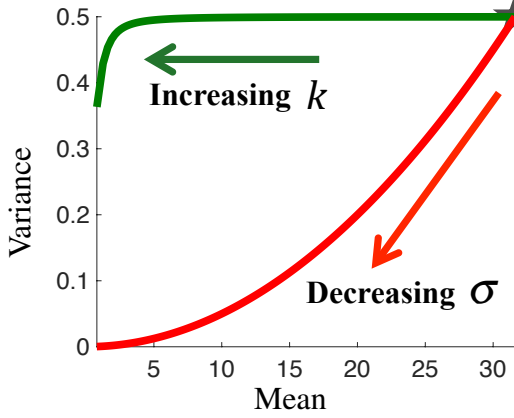


Figure 1. Starting from radius distribution in Equation (10) with $d = 100$, $\sigma = 1$ and $k = 0$ (black star), increasing k (green curve) allows us to move the mean towards zero *without significantly reducing the variance*. Decreasing σ (red curve) can also decrease the mean, but with a cost of decreasing the variance quadratically.

Computational Method With the more general centripetal smoothing distribution, we no longer have the closed-form solution of the bound like Equation (8) and Equation (7). However, efficient computational methods can still be developed for calculating the bound in Equation (6) with π_0 in Equation (10). The key is that the maximum of the distance term $\mathbb{D}_{\mathcal{F}_{[0,1]}}(\lambda\pi_0 \parallel \pi_\delta)$ over $\delta \in \mathcal{B}$ is always achieved on the boundary of \mathcal{B} as we show in the sequel, while the optimization on $\lambda \geq 0$ is one-dimensional and can be solved numerically efficiently.

Theorem 2. Consider the ℓ_1 attack with $\mathcal{B} = \{\delta : \|\delta\|_1 \leq r\}$ and smoothing distribution $\pi_0(\mathbf{z}) \propto \|\mathbf{z}\|_1^{-k} \exp\left(-\frac{\|\mathbf{z}\|_1}{b}\right)$ with $k \geq 0$ and $b > 0$, or the ℓ_2 attack with $\mathcal{B} = \{\delta : \|\delta\|_2 \leq r\}$ and smoothing distribution $\pi_0(\mathbf{z}) \propto \|\mathbf{z}\|_2^{-k} \exp\left(-\frac{\|\mathbf{z}\|_2^2}{2\sigma^2}\right)$ with $k \geq 0$ and $\sigma > 0$. Define $\delta^* = [r, 0, \dots, 0]^\top$, we have

$$\mathbb{D}_{\mathcal{F}_{[0,1]}}(\lambda\pi_0 \parallel \pi_{\delta^*}) = \max_{\delta \in \mathcal{B}} \mathbb{D}_{\mathcal{F}_{[0,1]}}(\lambda\pi_0 \parallel \pi_\delta)$$

for any positive λ .

The complete proof is in Appendix. With Theorem 2, we can compute Equation (6) with $\delta = \delta^*$. We then calculate $\mathbb{D}_{\mathcal{F}_{[0,1]}}(\lambda\pi_0 \parallel \pi_{\delta^*})$ using Monte Carlo approximation. Note that

$$\mathbb{D}_{\mathcal{F}_{[0,1]}}(\lambda\pi_0 \parallel \pi_{\delta^*}) = \mathbb{E}_{\mathbf{z} \sim \pi_0} \left[\left(\lambda - \frac{\pi_{\delta^*}(\mathbf{z})}{\pi_0(\mathbf{z})} \right)_+ \right],$$

which can be approximated with Monte Carlo method with Hoeffding concentration bound. Let $\{\mathbf{z}_i\}_{i=1}^n$ be i.i.d. sam-

ples from π_0 , then we approximate $\mathbb{D}_{\mathcal{F}_{[0,1]}}(\lambda\pi_0 \parallel \pi_{\delta^*})$ with

$$\hat{D} := \frac{1}{n} \sum_{i=1}^n (\lambda - \pi_{\delta^*}(\mathbf{z}_i)/\pi_0(\mathbf{z}_i))_+.$$

As a result of $0 \leq (\lambda - \pi_{\delta^*}(\mathbf{z}_i)/\pi_0(\mathbf{z}_i))_+ \leq \lambda$, $\mathbb{D}_{\mathcal{F}_{[0,1]}}(\lambda\pi_0 \parallel \pi_{\delta^*})$ will range in the following confidence interval

$$[\hat{D} - \lambda\sqrt{\log(2/\delta)/(2n)}, \hat{D} + \lambda\sqrt{\log(2/\delta)/(2n)}]$$

with confidence level $1 - \delta$ for $\delta \in (0, 1)$. Drawing a sufficiently large number of samples allows us to achieve approximation with arbitrary accuracy.

4.3. ℓ_∞ Region Certification

Going beyond the ℓ_1 and ℓ_2 attack, we consider the ℓ_∞ attack, whose attacking region is $\mathcal{B}_{\ell_\infty, r} = \{\delta : \|\delta\|_\infty \leq r\}$. The commonly used Gaussian smoothing distribution, as well as our ℓ_2 -based smoothing distribution in Equation (10), is unsuitable for this region.

Corollary 3. With the smoothing distribution π_0 in Equation (10) for $k \geq 0, \sigma > 0$, and $\mathcal{F} = \mathcal{F}_{[0,1]}$ shown in Equation (4), the bound we get for certifying the ℓ_∞ attack on $\mathcal{B}_{\ell_\infty, r} = \{\delta : \|\delta\|_\infty \leq r\}$ is equivalent to that for certifying the ℓ_2 attack on $\mathcal{B}_{\ell_2, \sqrt{d}r} = \{\delta : \|\delta\|_2 \leq \sqrt{d}r\}$, that is,

$$\mathcal{L}_{\pi_0}(\mathcal{F}_{[0,1]}, \mathcal{B}_{\ell_\infty, r}) = \mathcal{L}_{\pi_0}(\mathcal{F}_{[0,1]}, \mathcal{B}_{\ell_2, \sqrt{d}r}).$$

As shown in this corollary, if we use Equation (10) as the smoothing distribution for ℓ_∞ attack, the bound we obtain is effectively the bound we would get for verifying a ℓ_2 ball with radius $\sqrt{d}r$, which is too large to give meaningful results when the dimension is high. The maximum distance $\max_{\delta \in \mathcal{B}_{\ell_\infty, r}} \mathbb{D}_{\mathcal{F}}(\lambda\pi_0 \parallel \pi_\delta)$ is achieved at one of these pointy points, i.e., $\delta^* = [\sqrt{d}r, 0, \dots, 0]^\top$, making it equivalent to optimizing in the ℓ_2 ball with radius $\sqrt{d}r$.

In order to address this problem, we extend our proposed distribution family with new distributions which are more suitable for ℓ_∞ certification setting. We propose the following two new smoothing distributions for ℓ_∞ certification:

$$\pi_0(\mathbf{z}) \propto \|\mathbf{z}\|_\infty^{-k} \exp\left(-\frac{\|\mathbf{z}\|_\infty^2}{2\sigma^2}\right), \quad (12)$$

$$\pi_0(\mathbf{z}) \propto \|\mathbf{z}\|_\infty^{-k} \exp\left(-\frac{\|\mathbf{z}\|_2^2}{2\sigma^2}\right). \quad (13)$$

The motivation is to allocate more probability mass along the “pointy” directions with larger ℓ_∞ norm, and hence decrease the maximum distance term $\max_{\delta \in \mathcal{B}_{\ell_\infty, r}} \mathbb{D}_{\mathcal{F}}(\lambda\pi_0 \parallel \pi_\delta)$, see Figure 2 for illumination.

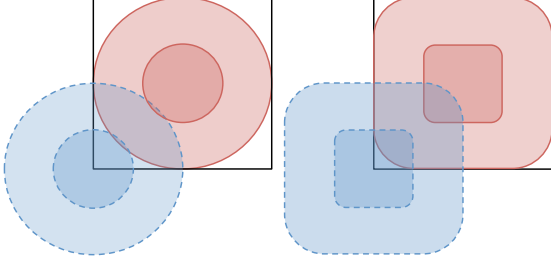


Figure 2. For ℓ_∞ attacking, compared with the distribution in Equation (10), the mixed norm distribution in Equation (13) (right) yields smaller discrepancy term (because of larger overlap areas), and hence higher robustness and better confidence bound. The distribution described in Equation (12) has the same impact.

Computational Method In order to compute the lower bound when using Equation (12) and Equation (13), we need to establish the closed form solution of the maximum distance term $\max_{\delta \in \mathcal{B}} \mathbb{D}_{\mathcal{F}_{[0,1]}}(\lambda \pi_0 \parallel \pi_\delta)$, which is similar to Theorem 2. The following result shows that the optimal δ is achieved at one vertex (the pointy points) of the ℓ_∞ ball.

Theorem 3. Consider the ℓ_∞ attack with $\mathcal{B}_{\ell_\infty, r} = \{\delta : \|\delta\|_\infty \leq r\}$ and the mixed norm smoothing distribution in Equation (13) with $k \geq 0$ and $\sigma > 0$. Define $\delta^* = [r, r, \dots, r]^\top$. We have for any $\lambda > 0$,

$$\mathbb{D}_{\mathcal{F}_{[0,1]}}(\lambda \pi_0 \parallel \pi_{\delta^*}) = \max_{\delta \in \mathcal{B}} \mathbb{D}_{\mathcal{F}_{[0,1]}}(\lambda \pi_0 \parallel \pi_\delta).$$

The proofs of Theorem 2 and 3 are non-trivial, thus we defer the details to the Appendix. With the optimal δ^* found above, we can calculate the bound with similar Monte Carlo approximation outlined in Section 4.2.

5. Experiments

We evaluate our new certification bound and smoothing distributions for ℓ_1 , ℓ_2 and ℓ_∞ attacks. We compare with the randomized smoothing method of Teng et al. (2020) with Laplacian smoothing for ℓ_1 region certification. For ℓ_2 and ℓ_∞ cases, we regard the method derived by Cohen et al. (2019) with Gaussian smoothing distribution as the baseline. For fair comparisons, we use the same model architecture and pre-trained models provided by Teng et al. (2020), Cohen et al. (2019) and Salman et al. (2019), which are ResNet-110 for CIFAR-10 and ResNet-50 for ImageNet. We defer more details, hyperparameters, and the settings to the Appendix B.1.

Evaluation Metrics The methods are evaluated using the certified accuracy defined in Cohen et al. (2019). Given an input image x and a perturbation region \mathcal{B} , the smoothed

classifier certifies image x correctly if the prediction is correct and has a guaranteed confidence lower bound larger than $1/2$ for any $\delta \in \mathcal{B}$. The certified accuracy is the percentage of images that are certified correctly. Following Salman et al. (2019), we calculate the certified accuracy of all the classifiers in Cohen et al. (2019) or Salman et al. (2019) for various radius, and report the best results over all of classifiers. We use the official code¹ provided by Cohen et al. (2019) for all the following experiments.

5.1. ℓ_1 Certification

We compare our method with Teng et al. (2020) on CIFAR-10 and ImageNet for ℓ_1 certification with the type 1 trained model in Teng et al. (2020). As shown in Table 1, our non-Laplacian centripetal distribution consistently outperforms the result of Teng et al. (2020) for any radius, e.g., for the radius 1.0, our proposed distribution in Equation (11) is able to improve the original baseline accuracy from 23% to 27%.

ℓ_1 RADIUS	0.25	0.5	0.75	1.0	1.25	1.5	1.75	2.0	2.25
BASELINE (%)	62	49	38	30	23	19	17	14	12
OURS (%)	64	51	41	34	27	22	18	17	14

Table 1. Certified top-1 accuracy of the best classifiers with various ℓ_1 radius on CIFAR-10.

We summarize the result on ImageNet in Table 2, which shows that our method outperforms the baseline’s result uniformly for all ℓ_1 radius.

ℓ_1 RADIUS	0.5	1.0	1.5	2.0	2.5	3.0	3.5
BASELINE (%)	50	41	33	29	25	18	15
OURS (%)	51	42	36	30	26	22	16

Table 2. Certified top-1 accuracy of the best classifiers with various ℓ_1 radius on ImageNet.

5.2. ℓ_2 Certification

We compare our method with Cohen et al. (2019) on CIFAR-10 and ImageNet for ℓ_2 certification. For a fair comparison, we use the same pre-trained models as Cohen et al. (2019), which is trained with Gaussian noise on both CIFAR-10 and ImageNet dataset. Table 3 and Table 4 report the certified accuracy of our method and the baseline on CIFAR-10 and ImageNet respectively. We find that our method consistently outperforms the baseline. Since we fix the same k across all the models and all the radius, the improvement cannot be obtained by tuning σ^2 fine-grainedly. The readers are referred to the Appendix C for detailed ablation studies.

¹<https://github.com/locuslab/smoothing>

ℓ_2 RADIUS	0.25	0.5	0.75	1.0	1.25	1.5	1.75	2.0	2.25
BASELINE (%)	60	43	34	23	17	14	12	10	8
OURS (%)	61	46	37	25	19	16	14	11	9

Table 3. Certified top-1 accuracy of the best classifiers with various ℓ_2 radius on CIFAR-10.

ℓ_2 RADIUS	0.5	1.0	1.5	2.0	2.5	3.0	3.5
BASELINE (%)	49	37	29	19	15	12	9
OURS (%)	50	39	31	21	17	13	10

Table 4. Certified top-1 accuracy of the best classifiers with various ℓ_2 radius on ImageNet.

5.3. ℓ_∞ Certification

Toy Example We first construct a simple toy example to verify the advantages of the distribution Equation (13) and Equation (12) over the ℓ_2 family in Equation (10).

We assume that the true classifier is $f^\#(\mathbf{x}) = \mathbb{I}(\|\mathbf{x}\|_2 \leq r)$ in $r = 0.65$, $d = 5$ case and plot in Figure 3 the Pareto frontier of the accuracy and robustness terms in Equation (9) for the three families of smoothing distributions, as we search for the best combinations of parameters (k, σ) . We can see that the mixed norm smoothing distribution clearly obtain the best trade-off on accuracy and robustness, and hence guarantees a tighter lower bound for certification. Figure 3 also shows that the distribution in Equation (12) even performs worse than the distribution described in Equation (10). We further prove that Equation (12) is provably not suitable for ℓ_∞ region certification in Appendix A.5.

ℓ_∞ RADIUS	2/255	4/255	6/255	8/255	10/255	12/255
BASELINE (%)	58	42	31	25	18	13
OURS (%)	60	47	38	32	23	17

Table 5. Certified top-1 accuracy of the best classifiers with various ℓ_∞ radius on CIFAR-10.

CIFAR-10 Based on the conclusion of the toy case, we only compared the method defined by Equation (13) with Salman et al. (2019) on CIFAR-10 using the models trained by Salman et al. (2019). The certified accuracy of our method and the baseline using Gaussian smoothing distribution and Corollary 3 are shown in Table 5. We can see that our method consistently outperforms the Gaussian distribution baseline by a large margin, which empirically shows our distribution is a more suitable distribution for ℓ_∞ perturbation.

To further confirm the advantage of our method, we plot in Figure 4 the certified accuracy of our method and Gaussian

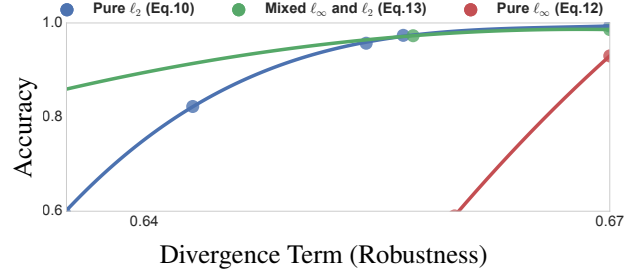


Figure 3. The Pareto frontier of accuracy and robustness (in the sense of Equation (9)) of the three smoothing families in Equation (10), Equation (13), and Equation (12) for ℓ_∞ attacking, when we search for the best parameters (k, σ) for each of them. The mixed norm family Equation (13) yields the best trade-off than the other two. We assume $f^\#(\mathbf{x}) = \mathbb{I}(\|\mathbf{x}\|_2 \leq r)$ and dimension $d = 5$. The case when $f^\#(\mathbf{x}) = \mathbb{I}(\|\mathbf{x}\|_\infty \leq r)$ has similar result (not shown).

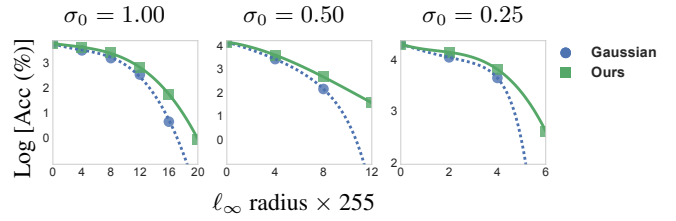


Figure 4. Results of ℓ_∞ verification on CIFAR-10, on models trained with Gaussian noise data augmentation with different variances σ_0 . Our method obtains consistently better results.

baseline using models trained with Gaussian perturbation of different variances σ_0 , under different ℓ_∞ radius. We again find that our approach outperforms the baseline consistently, especially when the ℓ_∞ radius is large. We also experimented our method and baseline on ImageNet, but did not obtain non-trivial results. This is because ℓ_∞ verification is extremely hard with very large dimensions. Future work will investigate how to obtain non-trivial bounds for ℓ_∞ attacking at ImageNet scales with smoothing classifiers.

6. Conclusion

We propose a general functional optimization based framework of adversarial certification with non-Gaussian smoothing distributions. Based on the insights from our new framework and high dimensional geometry, we propose a new family of non-Gaussian smoothing distributions, which outperform the Gaussian and Laplace smoothing for certifying ℓ_1 , ℓ_2 and ℓ_∞ attacking. Our work provides a basis for a variety of future directions, including improved methods for ℓ_p attacks, and tighter bounds based on adding additional constraints to our optimization framework.

References

- Athalye, A., Carlini, N., and Wagner, D. A. Obfuscated gradients give a false sense of security: Circumventing defenses to adversarial examples. pp. 274–283, 2018.
- Boyd, S. and Vandenberghe, L. *Convex Optimization*. Cambridge University Press, New York, NY, USA, 2004. ISBN 0521833787.
- Carlini, N., Katz, G., Barrett, C., and Dill, D. L. Provably minimally-distorted adversarial examples, 2017.
- Cheng, C., Nührenberg, G., and Ruess, H. Maximum resilience of artificial neural networks. In *Automated Technology for Verification and Analysis - 15th International Symposium, ATVA 2017, Pune, India, October 3-6, 2017, Proceedings*, pp. 251–268, 2017.
- Cohen, J. M., Rosenfeld, E., and Kolter, J. Z. Certified adversarial robustness via randomized smoothing. *arXiv preprint arXiv:1902.02918*, 2019.
- Deng, J., Dong, W., Socher, R., Li, L.-J., Li, K., and Fei-Fei, L. Imagenet: A large-scale hierarchical image database. In *2009 IEEE conference on computer vision and pattern recognition*, pp. 248–255. Ieee, 2009.
- Devlin, J., Chang, M., Lee, K., and Toutanova, K. BERT: pre-training of deep bidirectional transformers for language understanding. In *Proceedings of the 2019 Conference of the North American Chapter of the Association for Computational Linguistics: Human Language Technologies, NAACL-HLT 2019, Minneapolis, MN, USA, June 2-7, 2019, Volume 1 (Long and Short Papers)*, pp. 4171–4186, 2019. URL <https://www.aclweb.org/anthology/N19-1423/>.
- Dutta, S., Jha, S., Sankaranarayanan, S., and Tiwari, A. Output range analysis for deep feedforward neural networks, 2018.
- Dvijotham, K., Stanforth, R., Goyal, S., Mann, T. A., and Kohli, P. A dual approach to scalable verification of deep networks. In *Proceedings of the Thirty-Fourth Conference on Uncertainty in Artificial Intelligence, UAI 2018, Monterey, California, USA, August 6-10, 2018*, pp. 550–559, 2018. URL <http://auai.org/uai2018/proceedings/papers/204.pdf>.
- Dvijotham, K. D., Hayes, J., Balle, B., Kolter, Z., Qin, C., Gyorgy, A., Xiao, K., Goyal, S., and Kohli, P. A framework for robustness certification of smoothed classifiers using f-divergences. In *International Conference on Learning Representations*, 2020. URL <https://openreview.net/forum?id=SJlKrKSFPH>.
- Ehlers, R. Formal verification of piece-wise linear feed-forward neural networks. In *International Symposium on Automated Technology for Verification and Analysis*, pp. 269–286. Springer, 2017.
- Goodfellow, I. J., Shlens, J., and Szegedy, C. Explaining and harnessing adversarial examples. 2015.
- He, K., Zhang, X., Ren, S., and Sun, J. Deep residual learning for image recognition. In *Proceedings of the IEEE conference on computer vision and pattern recognition*, pp. 770–778, 2016.
- Jia, J., Cao, X., Wang, B., and Gong, N. Z. Certified robustness for top-k predictions against adversarial perturbations via randomized smoothing. In *International Conference on Learning Representations*, 2020. URL <https://openreview.net/forum?id=BkeWw6VFwr>.
- Jordan, M., Lewis, J., and Dimakis, A. G. Provable certificates for adversarial examples: Fitting a ball in the union of polytopes. *arXiv preprint arXiv:1903.08778*, 2019.
- Kannan, H., Kurakin, A., and Goodfellow, I. Adversarial logit pairing. *arXiv preprint arXiv:1803.06373*, 2018.
- Lecuyer, M., Atlidakis, V., Geambasu, R., Hsu, D., and Jana, S. Certified robustness to adversarial examples with differential privacy. *arXiv preprint arXiv:1802.03471*, 2018.
- Lee, G.-H., Yuan, Y., Chang, S., and Jaakkola, T. S. A stratified approach to robustness for randomly smoothed classifiers. *Advances in neural information processing systems (NeurIPS)*, 2019.
- Li, B., Chen, C., Wang, W., and Carin, L. Second-order adversarial attack and certifiable robustness. *Advances in neural information processing systems (NeurIPS)*, 2019.
- Li, W. V. and Kuelbs, J. Some shift inequalities for gaussian measures. In *High dimensional probability*, pp. 233–243. Springer, 1998.
- Liu, X., Cheng, M., Zhang, H., and Hsieh, C.-J. Towards robust neural networks via random self-ensemble. In *Proceedings of the European Conference on Computer Vision (ECCV)*, pp. 369–385, 2018.
- Madry, A., Makelov, A., Schmidt, L., Tsipras, D., and Vladu, A. Towards deep learning models resistant to adversarial attacks. 2018.
- Raghunathan, A., Steinhardt, J., and Liang, P. Semidefinite relaxations for certifying robustness to adversarial examples, 2018.

- Salman, H., Yang, G., Li, J., Zhang, P., Zhang, H., Razenshteyn, I., and Bubeck, S. Provably robust deep learning via adversarially trained smoothed classifiers. *arXiv preprint arXiv:1906.04584*, 2019.
- Szegedy, C., Zaremba, W., Sutskever, I., Bruna, J., Erhan, D., Goodfellow, I., and Fergus, R. Intriguing properties of neural networks. *arXiv preprint arXiv:1312.6199*, 2013.
- Teng, J., Lee, G.-H., and Yuan, Y. ℓ_1 adversarial robustness certificates: a randomized smoothing approach, 2020. URL <https://openreview.net/forum?id=H1lQIgrFDS>.
- Vershynin, R. *High-dimensional probability: An introduction with applications in data science*, volume 47. Cambridge University Press, 2018.
- Wang, D., Gong, C., and Liu, Q. Improving neural language modeling via adversarial training. pp. 6555–6565, 2019.
- Wong, E. and Kolter, J. Z. Provable defenses against adversarial examples via the convex outer adversarial polytope. *arXiv preprint arXiv:1711.00851*, 2017.
- Xie, C., Wang, J., Zhang, Z., Ren, Z., and Yuille, A. Mitigating adversarial effects through randomization, 2018.
- Zhai, R., Cai, T., He, D., Dan, C., He, K., Hopcroft, J., and Wang, L. Adversarially robust generalization just requires more unlabeled data. *arXiv preprint arXiv:1906.00555*, 2019.
- Zhang, D., Zhang, T., Lu, Y., Zhu, Z., and Dong, B. You only propagate once: Accelerating adversarial training via maximal principle. *Advances in neural information processing systems (NeurIPS)*, 2019.
- Zhang, H. and Wang, J. Defense against adversarial attacks using feature scattering-based adversarial training, 2019.
- Zhang, H., Weng, T.-W., Chen, P.-Y., Hsieh, C.-J., and Daniel, L. Efficient neural network robustness certification with general activation functions. In *Advances in neural information processing systems*, pp. 4939–4948, 2018.

A. Proofs

A.1. Proof for the strong duality in Theorem 1

We first introduce the following lemma, which is a straight forward generalization of the strong Lagrange duality to functional optimization case.

Lemma 4. *Given some δ^* , we have*

$$\begin{aligned} & \max_{\lambda \in \mathbb{R}} \min_{f \in \mathcal{F}_{[0,1]}} \mathbb{E}_{\pi_{\delta^*}} [f(\mathbf{x}_0 + \mathbf{z})] + \lambda (f_{\pi_0}^\#(\mathbf{x}_0) - \mathbb{E}_{\pi_0} [f(\mathbf{x}_0 + \mathbf{z})]) \\ &= \max_{\lambda \in \mathbb{R}} \min_{f \in \mathcal{F}_{[0,1]}} \mathbb{E}_{\pi_{\delta^*}} [f(\mathbf{x}_0 + \mathbf{z})] + \lambda (f_{\pi_0}^\#(\mathbf{x}_0) - \mathbb{E}_{\pi_0} [f(\mathbf{x}_0 + \mathbf{z})]) . \end{aligned}$$

The proof of Lemma 4 is standard. However, for completeness, we include it here.

Proof. Without loss of generality, we assume $f_{\pi_0}^\#(\mathbf{x}_0) \in (0, 1)$, otherwise the feasible set is trivial.

Let α^* be the value of the optimal solution of the primal problem. We define $f_{\pi_0}^\#(\mathbf{x}_0) - \mathbb{E}_{\pi_0} [f(\mathbf{x}_0 + \mathbf{z})] = h[f]$ and $g[f] = \mathbb{E}_{\pi_{\delta^*}} [f(\mathbf{x}_0 + \mathbf{z})]$. We define the following two sets:

$$\begin{aligned} \mathcal{A} &= \{(v, t) \in \mathbb{R} \times \mathbb{R} : \exists f \in \mathcal{F}_{[0,1]}, h[f] = v, g[f] \leq t\} \\ \mathcal{B} &= \{(0, s) \in \mathbb{R} \times \mathbb{R} : s < \alpha^*\} . \end{aligned}$$

Notice that both sets \mathcal{A} and \mathcal{B} are convex. This is obvious for \mathcal{B} . For any $(v_1, t_1) \in \mathcal{A}$ and $(v_2, t_2) \in \mathcal{A}$, we define $f_1 \in \mathcal{F}_{[0,1]}$ such that $h[f_1] = v_1, g[f_1] \leq t_1$ (and similarly we define f_2). Notice that for any $\gamma \in [0, 1]$, we have

$$\begin{aligned} \gamma f_1 + (1 - \gamma) f_2 &\in \mathcal{F}_{[0,1]} \\ \gamma h[f_1] + (1 - \gamma) h[f_2] &= \gamma v_1 + (1 - \gamma) v_2 \\ \gamma g[f_1] + (1 - \gamma) g[f_2] &\leq \gamma t_1 + (1 - \gamma) t_2, \end{aligned}$$

which implies that $\gamma(v_1, t_1) + (1 - \gamma)(v_2, t_2) \in \mathcal{A}$ and thus \mathcal{A} is convex. Also notice that by definition, $\mathcal{A} \cap \mathcal{B} = \emptyset$. Using separating hyperplane theorem, there exists a point $(q_1, q_2) \neq (0, 0)$ and a value α such that for any $(v, t) \in \mathcal{A}$, $q_1 v + q_2 t \geq \alpha$ and for any $(0, s) \in \mathcal{B}$, $q_2 s \leq \alpha$. Notice that we must have $q_2 \geq 0$, otherwise, for sufficient s , we will have $q_2 s > \alpha$. We thus have, for any $f \in \mathcal{F}_{[0,1]}$, we have

$$q_1 h[f] + q_2 g[f] \geq \alpha^* \geq q_2 \alpha^* .$$

If $q_2 > 0$, we have

$$\max_{\lambda \in \mathbb{R}} \min_{f \in \mathcal{F}_{[0,1]}} g[f] + \lambda h[f] \geq \min_{f \in \mathcal{F}_{[0,1]}} g[f] + \frac{q_1}{q_2} h[f] \geq \alpha^* ,$$

which gives the strong duality. If $q_2 = 0$, we have for any $f \in \mathcal{F}_{[0,1]}$, $q_1 h[f] \geq 0$ and by the separating hyperplane theorem, $q_1 \neq 0$. However, this case is impossible: If $q_1 > 0$, choosing $f \equiv 1$ gives $q_1 h[f] = q_1 (f_{\pi_0}^\#(\mathbf{x}_0) - 1) < 0$; If $q_1 < 0$, by choosing $f \equiv 0$, we have $q_1 h[f] = q_1 (f_{\pi_0}^\#(\mathbf{x}_0) - 0) < 0$. Both cases give contradiction. \square

Based on Lemma 4, we have the proof of the strong duality as follows.

Notice that by Lagrange multiplier method, our primal problem can be rewritten as follows:

$$\min_{\delta \in \mathcal{B}} \min_{f \in \mathcal{F}_{[0,1]}} \max_{\lambda \in \mathbb{R}} \mathbb{E}_{\pi_\delta} [f(\mathbf{x}_0 + \mathbf{z})] + \lambda (f_{\pi_0}^\#(\mathbf{x}_0) - \mathbb{E}_{\pi_0} [f(\mathbf{x}_0 + \mathbf{z})]) ,$$

and the dual problem is

$$\begin{aligned} & \max_{\lambda \in \mathbb{R}} \min_{\delta \in \mathcal{B}} \min_{f \in \mathcal{F}_{[0,1]}} \mathbb{E}_{\pi_\delta} [f(\mathbf{x}_0 + \mathbf{z})] + \lambda (f_{\pi_0}^\#(\mathbf{x}_0) - \mathbb{E}_{\pi_0} [f(\mathbf{x}_0 + \mathbf{z})]) \\ &= \max_{\lambda \geq 0} \min_{\delta \in \mathcal{B}} \min_{f \in \mathcal{F}_{[0,1]}} \mathbb{E}_{\pi_\delta} [f(\mathbf{x}_0 + \mathbf{z})] + \lambda (f_{\pi_0}^\#(\mathbf{x}_0) - \mathbb{E}_{\pi_0} [f(\mathbf{x}_0 + \mathbf{z})]) . \end{aligned}$$

By the assumption that for any $\lambda \geq 0$, we have

$$\begin{aligned} & \max_{\lambda \geq 0} \min_{\delta \in \mathcal{B}} \min_{f \in \mathcal{F}_{[0,1]}} \mathbb{E}_{\pi_\delta} [f(\mathbf{x}_0 + \mathbf{z})] + \lambda (f_{\pi_0}^\#(\mathbf{x}_0) - \mathbb{E}_{\pi_0} [f(\mathbf{x}_0 + \mathbf{z})]) \\ &= \max_{\lambda \geq 0} \min_{f \in \mathcal{F}_{[0,1]}} \mathbb{E}_{\pi_{\delta^*}} [f(\mathbf{x}_0 + \mathbf{z})] + \lambda (f_{\pi_0}^\#(\mathbf{x}_0) - \mathbb{E}_{\pi_0} [f(\mathbf{x}_0 + \mathbf{z})]), \end{aligned}$$

for some $\delta^* \in \mathcal{B}$. We have

$$\begin{aligned} & \max_{\lambda \in \mathbb{R}} \min_{\delta \in \mathcal{B}} \min_{f \in \mathcal{F}_{[0,1]}} \mathbb{E}_{\pi_\delta} [f(\mathbf{x}_0 + \mathbf{z})] + \lambda (f_{\pi_0}^\#(\mathbf{x}_0) - \mathbb{E}_{\pi_0} [f(\mathbf{x}_0 + \mathbf{z})]) \\ &= \max_{\lambda \geq 0} \min_{f \in \mathcal{F}_{[0,1]}} \mathbb{E}_{\pi_{\delta^*}} [f(\mathbf{x}_0 + \mathbf{z})] + \lambda (f_{\pi_0}^\#(\mathbf{x}_0) - \mathbb{E}_{\pi_0} [f(\mathbf{x}_0 + \mathbf{z})]) \\ &= \max_{\lambda \in \mathbb{R}} \min_{f \in \mathcal{F}_{[0,1]}} \mathbb{E}_{\pi_{\delta^*}} [f(\mathbf{x}_0 + \mathbf{z})] + \lambda (f_{\pi_0}^\#(\mathbf{x}_0) - \mathbb{E}_{\pi_0} [f(\mathbf{x}_0 + \mathbf{z})]) \\ &\stackrel{*}{=} \min_{f \in \mathcal{F}_{[0,1]}} \max_{\lambda \in \mathbb{R}} \mathbb{E}_{\pi_{\delta^*}} [f(\mathbf{x}_0 + \mathbf{z})] + \lambda (f_{\pi_0}^\#(\mathbf{x}_0) - \mathbb{E}_{\pi_0} [f(\mathbf{x}_0 + \mathbf{z})]) \\ &\geq \min_{\delta \in \mathcal{B}} \min_{f \in \mathcal{F}_{[0,1]}} \max_{\lambda \in \mathbb{R}} \mathbb{E}_{\pi_{\delta^*}} [f(\mathbf{x}_0 + \mathbf{z})] + \lambda (f_{\pi_0}^\#(\mathbf{x}_0) - \mathbb{E}_{\pi_0} [f(\mathbf{x}_0 + \mathbf{z})]), \end{aligned}$$

where the second equality (*) is by Lemma 4.

A.2. Proof for Corollary 1

Proof. Given our confidence lower bound

$$\max_{\lambda \geq 0} \min_{\|\delta\|_1 \leq r} \left\{ \lambda p_0 - \int (\lambda \pi_0(z) - \pi_\delta(z))_+ dz \right\},$$

One can show that the worst case for δ is obtained when $\delta^* = (r, 0, \dots, 0)$ (see following subsection), thus the bound is

$$\max_{\lambda \geq 0} \left\{ \lambda p_0 - \int \frac{1}{2b} \exp\left(-\frac{|z_1|}{b}\right) \left[\lambda - \exp\left(\frac{|z_1| - |z_1 + r|}{b}\right) \right]_+ dz_1 \right\}.$$

Denote a to be the solution of $\lambda = \exp\left(\frac{|a| - |a + r|}{b}\right)$, then obviously we have

$$a = \begin{cases} -\infty, & b \log \lambda \geq r \\ -\frac{1}{2}(b \log \lambda + r), & -r < b \log \lambda < r \\ +\infty. & b \log \lambda \leq -r \end{cases}$$

So the bound above is

$$\lambda \int_{z_1 > a} \frac{1}{2b} \exp\left(-\frac{|z_1|}{b}\right) dz_1 - \int_{z_1 > a} \frac{1}{2b} \exp\left(-\frac{|z_1 + r|}{b}\right) dz_1.$$

i) $b \log \lambda \geq r \Leftrightarrow \lambda \geq \exp\left(\frac{r}{b}\right)$

the bound is

$$\max_{\lambda \geq e^{r/b}} \{\lambda p_0 - (\lambda - 1)\} = 1 - \exp\left(\frac{r}{b}\right) (1 - p_0).$$

ii) $-r < b \log \lambda < r \Leftrightarrow \exp\left(-\frac{r}{b}\right) < \lambda < \exp\left(\frac{r}{b}\right)$

the bound is

$$\begin{aligned} & \max_{\lambda} \left\{ \lambda p_0 - \lambda \left[1 - \frac{1}{2} \exp\left(-\frac{b \log \lambda + r}{2b}\right) \right] + \frac{1}{2} \exp\left(\frac{b \log \lambda - r}{2b}\right) \right\} \\ &= \max_{\lambda} \left\{ \lambda(p_0 - 1) + \frac{\lambda}{2} \exp\left(-\frac{b \log \lambda + r}{2b}\right) + \frac{1}{2} \exp\left(\frac{b \log \lambda - r}{2b}\right) \right\} \\ &= \frac{1}{2} \exp\left(-\log[2(1 - p_0)] - \frac{r}{b}\right). \end{aligned}$$

the extremum is achieved when $\hat{\lambda} = \exp(-2 \log[2(1-p_0)] - \frac{r}{b})$. Notice that $\hat{\lambda}$ does not necessarily locate in $(e^{-r/b}, e^{r/b})$, so the actual bound is always equal or less than $\frac{1}{2} \exp(-\log[2(1-p_0)] - \frac{r}{b})$.

iii) $b \log \lambda \leq -r \Leftrightarrow \lambda \leq \exp(-\frac{r}{b})$
the bound is

$$\max_{\lambda \leq \exp(-\frac{r}{b})} \lambda \cdot p_0 = p_0 \exp\left(-\frac{r}{b}\right).$$

Since $\hat{\lambda} > e^{r/b} \Leftrightarrow p_0 > 1 - \frac{1}{2} \exp(-\frac{r}{b})$, notice that the lower bound is a concave function w.r.t. λ , making the final lower bound become

$$\begin{cases} 1 - \exp\left(\frac{r}{b}\right)(1-p_0), & \text{when } p_0 > 1 - \frac{1}{2} \exp(-\frac{r}{b}) \\ \frac{1}{2} \exp\left(-\log[2(1-p_0)] - \frac{r}{b}\right), & \text{otherwise} \end{cases}$$

□

Remark Actually, we have $1 - \exp\left(\frac{r}{b}\right)(1-p_0) \leq \frac{1}{2} \exp\left(-\log[2(1-p_0)] - \frac{r}{b}\right)$ all the time. Another interesting thing is that both the bound can lead to the same radius bound:

$$\begin{aligned} 1 - \exp\left(\frac{r}{b}\right)(1-p_0) &> \frac{1}{2} \Leftrightarrow r < -b \log[2(1-p_0)] \\ \frac{1}{2} \exp\left(-\log[2(1-p_0)] - \frac{r}{b}\right) &> \frac{1}{2} \Leftrightarrow r < -b \log[2(1-p_0)] \end{aligned}$$

A.3. Proof for Corollary 2

Proof. With strong duality, our confidence lower bound is

$$\min_{\|\delta\|_2 \leq r} \max_{\lambda \geq 0} \left\{ \lambda p_0 - \int (\lambda \pi_0(z) - \pi_\delta(z))_+ dz \right\},$$

define $C_\lambda = \{z : \lambda \pi_0(z) \geq \pi_\delta(z)\} = \{z : \delta^\top z \leq \frac{\|\delta\|_2^2}{2} + \sigma^2 \ln \lambda\}$ and $\Phi(\cdot)$ to be the cdf of standard gaussian distribution, then

$$\begin{aligned} &\int (\lambda \pi_0(z) - \pi_\delta(z))_+ dz \\ &= \int_{C_\lambda} (\lambda \pi_0(z) - \pi_\delta(z)) dz \\ &= \lambda \cdot \mathbb{P}(N(z; \mathbf{0}, \sigma^2 \mathbf{I}) \in C_\lambda) - \mathbb{P}(N(z; \delta, \sigma^2 \mathbf{I}) \in C_\lambda) \\ &= \lambda \cdot \Phi\left(\frac{\|\delta\|_2}{2\sigma} + \frac{\sigma \ln \lambda}{\|\delta\|_2}\right) - \Phi\left(\frac{-\|\delta\|_2}{2\sigma} + \frac{\sigma \ln \lambda}{\|\delta\|_2}\right). \end{aligned}$$

Define

$$F(\delta, \lambda) := \lambda p_0 - \int (\lambda \pi_0(z) - \pi_\delta(z))_+ dz = \lambda p_0 - \lambda \cdot \Phi\left(\frac{\|\delta\|_2}{2\sigma} + \frac{\sigma \ln \lambda}{\|\delta\|_2}\right) + \Phi\left(\frac{-\|\delta\|_2}{2\sigma} + \frac{\sigma \ln \lambda}{\|\delta\|_2}\right).$$

For $\forall \delta$, F is a concave function w.r.t. λ , as F is actually a summation of many concave piece wise linear function. See [Boyd & Vandenberghe \(2004\)](#) for more discussions of properties of concave functions.

Define $\hat{\lambda}_\delta = \exp\left(\frac{2\sigma\|\delta\|_2\Phi^{-1}(p_0) - \|\delta\|_2^2}{2\sigma^2}\right)$, simple calculation can show $\frac{\partial F(\delta, \lambda)}{\partial \lambda}|_{\lambda=\hat{\lambda}_\delta} = 0$, which means

$$\begin{aligned}
 \min_{\|\delta\|_2 \leq r} \max_{\lambda \geq 0} F(\delta, \lambda) &= \min_{\|\delta\|_2 \leq r} F(\delta, \lambda_\delta) \\
 &= \min_{\|\delta\|_2 \leq r} \left\{ 0 + \Phi \left(\frac{-\|\delta\|_2}{2\sigma} + \frac{\sigma \ln \hat{\lambda}_\delta}{\|\delta\|_2} \right) \right\} \\
 &= \min_{\|\delta\|_2 \leq r} \Phi \left(\Phi^{-1}(p_0) - \frac{\|\delta\|_2}{\sigma} \right) \\
 &= \Phi \left(\Phi^{-1}(p_0) - \frac{r}{\sigma} \right)
 \end{aligned}$$

This tells us

$$\min_{\|\delta\|_2 \leq r} \max_{\lambda \geq 0} F(\delta, \lambda) > 1/2 \Leftrightarrow \Phi \left(\Phi^{-1}(p_0) - \frac{r}{\sigma} \right) > 1/2 \Leftrightarrow r < \sigma \cdot \Phi^{-1}(p_0),$$

i.e. the certification radius is $\sigma \cdot \Phi^{-1}(p_0)$. This is exactly the core theoretical contribution of [Cohen et al. \(2019\)](#). This bound has a straight forward expansion for multi-class classification situations, we refer interesting readers to [Appendix D](#). \square

A.4. Proof For Theorem 2 and 3

A.4.1. PROOF FOR ℓ_2 AND ℓ_∞ CASES

Here we consider a more general smooth distribution $\pi_0(z) \propto \|z\|_\infty^{-k_1} \|z\|_2^{-k_2} \exp\left(-\frac{\|z\|_2^2}{2\sigma^2}\right)$, for some $k_1, k_2 \geq 0$ and $\sigma > 0$. We first gives the following key theorem shows that $\mathbb{D}_{\mathcal{F}_{[0,1]}}(\lambda\pi_0 \parallel \pi_\delta)$ increases as $|\delta_i|$ becomes larger for every dimension i .

Theorem 4. Suppose $\pi_0(z) \propto \|z\|_\infty^{-k_1} \|z\|_2^{-k_2} \exp\left(-\frac{\|z\|_2^2}{2\sigma^2}\right)$, for some $k_1, k_2 \geq 0$ and $\sigma > 0$, for any $\lambda \geq 0$ we have

$$\text{sgn}(\delta_i) \frac{\partial}{\partial \delta_i} \mathbb{D}_{\mathcal{F}_{[0,1]}}(\lambda\pi_0 \parallel \pi_\delta) \geq 0,$$

for any $i \in \{1, 2, \dots, d\}$.

Theorem 2 and 3 directly follows the above theorem. Notice that in Theorem 2, as our distribution is spherical symmetry, it is equivalent to set $\mathcal{B} = \{\delta : \delta = [a, 0, \dots, 0]^\top, a \leq r\}$ by rotating the axis.

Proof. Given λ, k_1 and k_2 , we define $\phi_1(s) = s^{-k_1}$, $\phi_2(s) = s^{-k_2} e^{-\frac{s^2}{2\sigma^2}}$. Notice that ϕ_1 and ϕ_2 are monotone decreasing for non-negative s . By the symmetry, without loss of generality, we assume $\delta = [\delta_1, \dots, \delta_d]^\top$ for $\delta_i \geq 0, i \in [d]$. Notice that

$$\begin{aligned}
 \frac{\partial}{\partial \delta_i} \|\mathbf{x}_0 - \delta\|_\infty &= \mathbb{I}\{\|\mathbf{x}_0 - \delta\|_\infty = |x_i - \delta_i|\} \frac{\partial}{\partial \delta_i} \sqrt{(x_i - \delta_i)^2} \\
 &= \mathbb{I}\{\|\mathbf{x}_0 - \delta\|_\infty = |x_i - \delta_i|\} \frac{-(x_i - \delta_i)}{\|\mathbf{x}_0 - \delta\|_\infty}.
 \end{aligned}$$

And also

$$\begin{aligned}
 \frac{\partial}{\partial \delta_i} \|\mathbf{x}_0 - \mu\|_2 &= \frac{\partial}{\partial \delta_i} \sqrt{\sum_i (x_i - \mu_i)^2} \\
 &= \frac{-(x_i - \mu_i)}{\|\mathbf{x}_0 - \mu\|_2}.
 \end{aligned}$$

We thus have

$$\begin{aligned}
 & \frac{\partial}{\partial \delta_1} \int (\lambda \pi_0(\mathbf{x}_0) - \pi_\delta(\mathbf{x}_0))_+ d\mathbf{x}_0 \\
 &= - \int \mathbb{I}\{\lambda \pi_0(\mathbf{x}_0) \geq \pi_\delta(\mathbf{x}_0)\} \frac{\partial}{\partial \delta_1} \pi_\delta(\mathbf{x}_0) d\mathbf{x}_0 \\
 &= \int \mathbb{I}\{\lambda \pi_0(\mathbf{x}_0) \geq \pi_\delta(\mathbf{x}_0)\} F_1(\|\mathbf{x}_0 - \boldsymbol{\delta}\|_\infty, \|\mathbf{x}_0 - \boldsymbol{\delta}\|_2) d\mathbf{x}_0 \\
 &= \int \mathbb{I}\{\lambda \pi_0(\mathbf{x}_0) \geq \pi_\delta(\mathbf{x}_0), x_1 > \delta_1\} F_1(\|\mathbf{x}_0 - \boldsymbol{\delta}\|_\infty, \|\mathbf{x}_0 - \boldsymbol{\delta}\|_2) d\mathbf{x}_0 \\
 &+ \int \mathbb{I}\{\lambda \pi_0(\mathbf{x}_0) \geq \pi_\delta(\mathbf{x}_0), x_1 < \delta_1\} F_1(\|\mathbf{x}_0 - \boldsymbol{\delta}\|_\infty, \|\mathbf{x}_0 - \boldsymbol{\delta}\|_2) d\mathbf{x}_0,
 \end{aligned}$$

where we define

$$\begin{aligned}
 & F_1(\|\mathbf{x}_0 - \boldsymbol{\delta}\|_\infty, \|\mathbf{x}_0 - \boldsymbol{\delta}\|_2) \\
 &= \phi'_1(\|\mathbf{x}_0 - \boldsymbol{\delta}\|_\infty) \phi_2(\|\mathbf{x}_0 - \boldsymbol{\delta}\|_2) \mathbb{I}\{\|\mathbf{x}_0 - \boldsymbol{\delta}\|_\infty = |x_1 - \delta_1|\} \frac{(x_1 - \delta_1)}{\|\mathbf{x}_0 - \boldsymbol{\delta}\|_\infty} \\
 &+ \phi_1(\|\mathbf{x}_0 - \boldsymbol{\delta}\|_\infty) \phi'_2(\|\mathbf{x}_0 - \boldsymbol{\delta}\|_2) \frac{(x_1 - \delta_1)}{\|\mathbf{x}_0 - \boldsymbol{\delta}\|_2}.
 \end{aligned}$$

Notice that as $\phi'_1 \leq 0$ and $\phi'_2 \leq 0$ and we have

$$\begin{aligned}
 & \int \mathbb{I}\{\lambda \pi_0(\mathbf{x}_0) \geq \pi_\delta(\mathbf{x}_0), x_1 > \delta_1\} F_1(\|\mathbf{x}_0 - \boldsymbol{\delta}\|_\infty, \|\mathbf{x}_0 - \boldsymbol{\delta}\|_2) d\mathbf{x}_0 \leq 0 \\
 & \int \mathbb{I}\{\lambda \pi_0(\mathbf{x}_0) \geq \pi_\delta(\mathbf{x}_0), x_1 < \delta_1\} F_1(\|\mathbf{x}_0 - \boldsymbol{\delta}\|_\infty, \|\mathbf{x}_0 - \boldsymbol{\delta}\|_2) d\mathbf{x}_0 \geq 0.
 \end{aligned}$$

Our target is to prove that $\frac{\partial}{\partial \delta_1} \int (\lambda \pi_0(\mathbf{x}_0) - \pi_\delta(\mathbf{x}_0))_+ d\mathbf{x}_0 \geq 0$. Now define the set

$$\begin{aligned}
 H_1 &= \{\mathbf{x}_0 : \lambda \pi_0(\mathbf{x}_0) \geq \pi_\delta(\mathbf{x}_0), x_1 > \delta_1\} \\
 H_2 &= \{[2\delta_1 - x_1, x_2, \dots, x_d]^\top : \mathbf{x}_0 = [x_1, \dots, x_d]^\top \in H_1\}.
 \end{aligned}$$

Here the set H_2 is defined as a image of a bijection

$$\text{proj}(\mathbf{x}_0) = [2\delta_1 - x_1, x_2, \dots, x_d]^\top = \tilde{\mathbf{x}}_0,$$

that is constrained on the set H_1 . Notice that under our definition,

$$\begin{aligned}
 & \int \mathbb{I}\{\lambda \pi_0(\mathbf{x}_0) \geq \pi_\delta(\mathbf{x}_0), x_1 > \delta_1\} F_1(\|\mathbf{x}_0 - \boldsymbol{\delta}\|_\infty, \|\mathbf{x}_0 - \boldsymbol{\delta}\|_2) d\mathbf{x}_0 \\
 &= \int_{H_1} F_1(\|\mathbf{x}_0 - \boldsymbol{\delta}\|_\infty, \|\mathbf{x}_0 - \boldsymbol{\delta}\|_2) d\mathbf{x}_0.
 \end{aligned}$$

Now we prove that

$$\begin{aligned}
 & \int \mathbb{I}\{\lambda \pi_0(\mathbf{x}_0) \geq \pi_\delta(\mathbf{x}_0), x_1 < \delta_1\} F_1(\|\mathbf{x}_0 - \boldsymbol{\delta}\|_\infty, \|\mathbf{x}_0 - \boldsymbol{\delta}\|_2) d\mathbf{x}_0 \\
 & \stackrel{(1)}{\geq} \int_{H_2} F_1(\|\mathbf{x}_0 - \boldsymbol{\delta}\|_\infty, \|\mathbf{x}_0 - \boldsymbol{\delta}\|_2) d\mathbf{x}_0 \\
 & \stackrel{(2)}{=} \left| \int_{H_1} F_1(\|\mathbf{x}_0 - \boldsymbol{\delta}\|_\infty, \|\mathbf{x}_0 - \boldsymbol{\delta}\|_2) d\mathbf{x}_0 \right|.
 \end{aligned}$$

Property of the projection Before we prove the (1) and (2), we give the following property of the defined projection function. For any $\tilde{x}_0 = \text{proj}(x_0)$, $x_0 \in H_1$, we have

$$\begin{aligned}\|x_0 - \delta\|_\infty &= \|\tilde{x}_0 - \delta\|_\infty \\ \|x_0 - \delta\|_2 &= \|\tilde{x}_0 - \delta\|_2 \\ \|x_0\|_2 &\geq \|\tilde{x}_0\|_2 \\ \|x_0\|_\infty &\geq \|\tilde{x}_0\|_\infty.\end{aligned}$$

This is because

$$\begin{aligned}\tilde{x}_i &= x_i, i \in [d] - \{1\} \\ \tilde{x}_1 &= 2\delta_1 - x_1,\end{aligned}$$

and by the fact that $x_1 \geq \delta_1 \geq 0$, we have $|\tilde{x}_1| \leq |x_1|$ and $|\tilde{x}_1 - \delta_1| \leq |x_1 - \delta_1|$.

Proof of Equality (2) By the fact that proj is bijective constrained on the set H_1 and the property of proj , we have

$$\begin{aligned}& \int_{H_2} F_1(\|\tilde{x}_0 - \delta\|_\infty, \|\tilde{x}_0 - \delta\|_2) d\tilde{x}_0 \\ &= \int_{H_2} \phi'_1(\|\tilde{x}_0 - \delta\|_\infty) \phi_2(\|\tilde{x}_0 - \delta\|_2) \mathbb{I}\{\|\tilde{x}_0 - \delta\|_\infty = |\tilde{x}_1 - \delta_1|\} \frac{(\tilde{x}_1 - \delta_1)}{\|\tilde{x}_0 - \delta\|_\infty} d\tilde{x}_0 \\ &+ \int_{H_2} \phi_1(\|\tilde{x}_0 - \delta\|_\infty) \phi'_2(\|\tilde{x}_0 - \delta\|_2) \frac{(\tilde{x}_1 - \delta_1)}{\|\tilde{x}_0 - \delta\|_2} d\tilde{x}_0 \\ &\stackrel{(*)}{=} \int_{H_1} \phi'_1(\|x_0 - \delta\|_\infty) \phi_2(\|x_0 - \delta\|_2) \mathbb{I}\{\|x_0 - \delta\|_\infty = |x_1 - \delta_1|\} \frac{(\delta_1 - x_1)}{\|x_0 - \delta\|_\infty} |\det(\mathbf{J})| dx_0 \\ &+ \int_{H_1} \phi_1(\|x_0 - \delta\|_\infty) \phi'_2(\|x_0 - \delta\|_2) \frac{(\delta_1 - x_1)}{\|x_0 - \delta\|_2} dx_0 \\ &= - \int_{H_1} F_1(\|x_0 - \delta\|_\infty, \|x_0 - \delta\|_2) dx_0,\end{aligned}$$

where $(*)$ is by change of variable $\tilde{x}_0 = \text{proj}(x_0)$ and \mathbf{J} is the Jacobian matrix $\mathbf{J} = \begin{bmatrix} -1 & 0 & \cdots & 0 \\ 0 & 1 & \cdots & 0 \\ \vdots & \vdots & \ddots & \vdots \\ 0 & 0 & \cdots & 1 \end{bmatrix}$ and here we

have the fact that $\tilde{x}_1 - \delta_1 = (2\delta_1 - x_1) - \delta_1 = -(x_1 - \delta_1)$.

Proof of Inequality (1) This can be done by verifying that $H_2 \subseteq \{x_0 : \lambda\pi_0(x_0) \geq \pi_\delta(x_0), x_1 < \delta_1\}$. By the property of the projection, for any $x_0 \in H_1$, let $\tilde{x}_0 = \text{proj}(x_0)$, then $\lambda\pi_0(\tilde{x}_0) \geq \lambda\pi_0(x_0) \geq \pi_\delta(x_0) = \pi_\delta(\tilde{x}_0)$ (by the fact that ϕ_1 and ϕ_2 are monotone decreasing). It implies that for any $\tilde{x}_0 \in H_2$, we have $\lambda\pi_0(\tilde{x}_0) \geq \pi_\delta(\tilde{x}_0)$ and thus $H_2 \subseteq \{x_0 : \pi_0(x_0) \geq \pi_\delta(x_0), x_1 < \delta_1\}$.

Final statement By the above result, we have

$$\frac{\partial}{\partial \delta_1} \int (\lambda\pi_0(x_0) - \pi_\delta(x_0))_+ dx_0 \geq 0,$$

and the same result holds for any $\frac{\partial}{\partial \delta_i} \int (\lambda\pi_0(x_0) - \pi_\delta(x_0))_+ dx_0, i \in [d]$, which implies our result. \square

A.4.2. PROOF FOR ℓ_1 CASE

Slightly different for former cases, apart from proving $\frac{\partial}{\partial \delta_i} \mathbb{D}_{\mathcal{F}_{[0,1]}}(\lambda\pi_0 \parallel \pi_\delta) \geq 0$ for $\forall \delta_i \geq 0$, we also need to demonstrate

Theorem 5. Suppose $\pi_0(x_0) \propto \|x_0\|^{-k} \exp\left(-\frac{\|x_0\|_1}{b}\right)$, then for $\delta = (r, d-r, \delta_3, \delta_4, \dots)$ and $\tilde{\delta} = (0, d, \delta_3, \delta_4, \dots)$, $0 < r < d$, we have

$$\mathbb{D}_{\mathcal{F}_{[0,1]}}(\lambda\pi_0 \parallel \pi_\delta) \geq \mathbb{D}_{\mathcal{F}_{[0,1]}}(\lambda\pi_0 \parallel \pi_{\tilde{\delta}})$$

Proof. We turn to show that

$$\frac{\partial}{\partial r} \mathbb{D}_{\mathcal{F}_{[0,1]}}(\lambda \pi_{\mathbf{0}} \parallel \pi_{\boldsymbol{\delta}}) \leq 0,$$

for $\boldsymbol{\delta} = (r, d-r, \delta_3, \delta_4, \dots)$ and $r < d/2$. We define $\phi(s) = s^{-k} \exp(-\frac{s}{b})$. With

$$\frac{\partial}{\partial \delta_i} \|\mathbf{x}_0 - \boldsymbol{\delta}\|_1 = \frac{\partial}{\partial \delta_i} |x_i - \delta_i| = -\text{sgn}(x_i - \delta_i) = \frac{\delta_i - x_i}{|x_i - \delta_i|},$$

We have

$$\begin{aligned} & \frac{\partial}{\partial r} \mathbb{D}_{\mathcal{F}_{[0,1]}}(\lambda \pi_{\mathbf{0}} \parallel \pi_{\boldsymbol{\delta}}) \\ &= - \int \mathbb{I}\{\lambda \pi_{\mathbf{0}}(\mathbf{x}_0) \geq \pi_{\boldsymbol{\delta}}(\mathbf{x}_0)\} \frac{\partial}{\partial r} \pi_{\boldsymbol{\delta}}(\mathbf{x}_0) d\mathbf{x}_0 \\ &= \int \mathbb{I}\{\lambda \pi_{\mathbf{0}}(\mathbf{x}_0) \geq \pi_{\boldsymbol{\delta}}(\mathbf{x}_0)\} F(\mathbf{x}_0) d\mathbf{x}_0, \end{aligned}$$

where

$$\begin{aligned} F(\mathbf{x}_0) &= - \frac{\partial}{\partial r} \phi(\|\mathbf{x}_0 - \boldsymbol{\delta}\|_1) = -\phi'(\|\mathbf{x}_0 - \boldsymbol{\delta}\|_1) \frac{\partial}{\partial r} \|\mathbf{x}_0 - \boldsymbol{\delta}\|_1 \\ &= \phi'(\|\mathbf{x}_0 - \boldsymbol{\delta}\|_1) \frac{\partial}{\partial r} (|x_1 - r| + |x_2 - d + r|) \\ &= \phi'(\|\mathbf{x}_0 - \boldsymbol{\delta}\|_1) \cdot (\text{sgn}(x_1 - r) + \text{sgn}(d - x_2 - r)). \end{aligned}$$

Thus the original derivative becomes

$$\begin{aligned} &= \int \mathbb{I}\{\lambda \pi_{\mathbf{0}}(\mathbf{x}_0) \geq \pi_{\boldsymbol{\delta}}(\mathbf{x}_0), x_1 > r, x_2 < d - r\} F(\mathbf{x}_0) d\mathbf{x}_0 \\ &\quad + \int \mathbb{I}\{\lambda \pi_{\mathbf{0}}(\mathbf{x}_0) \geq \pi_{\boldsymbol{\delta}}(\mathbf{x}_0), x_1 > r, x_2 > d - r\} F(\mathbf{x}_0) d\mathbf{x}_0 \\ &\quad + \int \mathbb{I}\{\lambda \pi_{\mathbf{0}}(\mathbf{x}_0) \geq \pi_{\boldsymbol{\delta}}(\mathbf{x}_0), x_1 < r, x_2 > d - r\} F(\mathbf{x}_0) d\mathbf{x}_0 \\ &\quad + \int \mathbb{I}\{\lambda \pi_{\mathbf{0}}(\mathbf{x}_0) \geq \pi_{\boldsymbol{\delta}}(\mathbf{x}_0), x_1 < r, x_2 < d - r\} F(\mathbf{x}_0) d\mathbf{x}_0 \\ &= 2 \int \mathbb{I}\{\lambda \pi_{\mathbf{0}}(\mathbf{x}_0) \geq \pi_{\boldsymbol{\delta}}(\mathbf{x}_0), x_1 > r, x_2 < d - r\} \phi'(\|\mathbf{x}_0 - \boldsymbol{\delta}\|_1) d\mathbf{x}_0 \\ &\quad - 2 \int \mathbb{I}\{\lambda \pi_{\mathbf{0}}(\mathbf{x}_0) \geq \pi_{\boldsymbol{\delta}}(\mathbf{x}_0), x_1 < r, x_2 > d - r\} \phi'(\|\mathbf{x}_0 - \boldsymbol{\delta}\|_1) d\mathbf{x}_0 \end{aligned}$$

We only need to show that

$$\int \mathbb{I}\{\lambda \pi_{\mathbf{0}}(\mathbf{x}_0) \geq \pi_{\boldsymbol{\delta}}(\mathbf{x}_0), x_1 > r, x_2 < d - r\} \phi'(\|\mathbf{x}_0 - \boldsymbol{\delta}\|_1) d\mathbf{x}_0 \geq \int \mathbb{I}\{\lambda \pi_{\mathbf{0}}(\mathbf{x}_0) \geq \pi_{\boldsymbol{\delta}}(\mathbf{x}_0), x_1 < r, x_2 > d - r\} \phi'(\|\mathbf{x}_0 - \boldsymbol{\delta}\|_1) d\mathbf{x}_0.$$

Notice that $r < d/2$, therefore this can be proved with a similar projection $\mathbf{x}_0 \mapsto \tilde{\mathbf{x}}_0$:

$$(x_1, x_2, x_3, x_4, \dots) \mapsto (2r - x_1, 2d - 2r - x_2, x_3, x_4, \dots)$$

and the similar deduction as previous theorem. □

A.5. Theoretical Demonstration about the Ineffativity of Equation (12)

Theorem 6. Consider the adversarial attacks on the ℓ_∞ ball $\mathcal{B}_{\ell_\infty, r} = \{\boldsymbol{\delta} : \|\boldsymbol{\delta}\|_\infty \leq r\}$. Suppose we use the smoothing distribution $\pi_{\mathbf{0}}$ in Equation (12) and choose the parameters (k, σ) such that

1) $\|z\|_\infty$ is stochastic bounded when $z \sim \pi_0$, in that for any $\epsilon > 0$, there exists a finite $M > 0$ such that $P_{\pi_0}(\|z\|_\infty > M) \leq \epsilon$;

2) the mode of $\|z\|_\infty$ under π_0 equals Cr , where C is some fixed positive constant,

then for any $\epsilon \in (0, 1)$ and sufficiently large dimension d , there exists a constant $t > 1$, such that, we have

$$\max_{\delta \in \mathcal{B}_{\ell_\infty, r}} \left\{ \mathbb{D}_{\mathcal{F}_{[0,1]}}(\lambda \pi_0 \parallel \pi_\delta) \right\} \geq (1 - \epsilon) (\lambda - \mathcal{O}(t^{-d})).$$

This shows that, in very high dimensions, the maximum distance term is arbitrarily close to λ which is the maximum possible value of $\mathbb{D}_{\mathcal{F}_{[0,1]}}(\lambda \pi_0 \parallel \pi_\delta)$ (see Theorem 1). In particular, this implies that in high dimensional scenario, once $f_{\pi_0}^\#(x_0) \leq (1 - \epsilon)$ for some small ϵ , we have $\mathcal{L}_{\pi_0}(\mathcal{F}_{[0,1]}, \mathcal{B}_{\ell_\infty, r}) = \mathcal{O}(t^{-d})$ and thus fail to certify.

Remark The condition 1) and 2) in Theorem 6 are used to ensure that the magnitude of the random perturbations generated by π_0 is within a reasonable range such that the value of $f_{\pi_0}^\#(x_0)$ is not too small, in order to have a high accuracy in the trade-off in Equation (9). Note that the natural images are often contained in cube $[0, 1]^d$. If $\|z\|_\infty$ is too large to exceed the region of natural images, the accuracy will be obviously rather poor. Note that if we use variants of Gaussian distribution, we only need $\|z\|_2/\sqrt{d}$ to be not too large. Theorem 6 says that once $\|z\|_\infty$ is in a reasonably small scale, the maximum distance term must be unreasonably large in high dimensions, yielding a vacuous lower bound.

Proof. First notice that the distribution of z can be factorized by the following hierarchical scheme:

$$\begin{aligned} a &\sim \pi_R(a) \propto a^{d-1-k} e^{-\frac{a^2}{2\sigma^2}} \mathbb{I}\{a \geq 0\} \\ s &\sim \text{Unif}^{\otimes d}(-1, 1) \\ z &\leftarrow \frac{s}{\|s\|_\infty} a. \end{aligned}$$

Without loss of generality, we assume $\delta^* = [r, \dots, r]^\top$. (see Theorem 4)

$$\mathbb{D}_{\mathcal{F}_{[0,1]}}(\lambda \pi_0 \parallel \pi_{\delta^*}) = \mathbb{E}_{z \sim \pi_0} \left(\lambda - \frac{\pi_\delta(z)}{\pi_0} \right)_+.$$

Notice that as the distribution is symmetry,

$$P_{\pi_0}(\|z + \delta^*\|_\infty = a + r \mid \|z\|_\infty = a) = \frac{1}{2}.$$

Define $|z|^{(i)}$ is the i -th order statistics of $|z_j|$, $j = 1, \dots, d$ conditioning on $\|z\|_\infty = a$. By the factorization above and some algebra, we have, for any $\epsilon \in (0, 1)$,

$$P \left(\frac{|z|^{(d-1)}}{|z|^{(d)}} > (1 - \epsilon) \mid \|z\|_\infty = a \right) \geq 1 - (1 - \epsilon)^{d-1}.$$

And $\frac{|z|^{(d-1)}}{|z|^{(d)}} \perp |z|^{(d)}$. Now we estimate $\mathbb{D}_{\mathcal{F}_{[0,1]}}(\lambda \pi_0 \parallel \pi_{\delta^*})$.

$$\begin{aligned} &\mathbb{E}_{z \sim \pi_0} \left(\lambda - \frac{\pi_\delta(z)}{\pi_0} \right)_+ \\ &= \mathbb{E}_a \mathbb{E}_{z \sim \pi_0} \left[\left(\lambda - \frac{\pi_\delta(z)}{\pi_0} \right)_+ \mid \|z\|_\infty = a \right] \\ &= \frac{1}{2} \mathbb{E}_a \mathbb{E}_{z \sim \pi_0} \left[\left(\lambda - \frac{\pi_\delta(z)}{\pi_0} \right)_+ \mid \|z\|_\infty = a, \|z + \delta^*\|_\infty = a + r \right] \\ &\quad + \frac{1}{2} \mathbb{E}_a \mathbb{E}_{z \sim \pi_0} \left[\left(\lambda - \frac{\pi_\delta(z)}{\pi_0} \right)_+ \mid \|z\|_\infty = a, \|z + \delta^*\|_\infty \neq a + r \right]. \end{aligned}$$

Conditioning on $\|z\|_\infty = a$, $\|z + \delta^*\|_\infty = a + r$, we have

$$\begin{aligned}\frac{\pi_\delta}{\pi_0}(z) &= \left(\frac{1}{1 + \frac{r}{a}}\right)^k e^{-\frac{1}{2\sigma^2}(2ra+r^2)} \\ &= \left(\frac{1}{1 + \frac{r}{a}}\right)^k e^{-\frac{d-1-k}{2C^2}(2\frac{a}{r}+1)}.\end{aligned}$$

Here the second equality is because we choose $\text{mode}(\|z\|_\infty) = Cr$, which implies that $\sqrt{d-1-k}\sigma = Cr$. And thus we have

$$\begin{aligned}&\mathbb{E}_a \mathbb{E}_{z \sim \pi_0} \left[\left(\lambda - \frac{\pi_\delta}{\pi_0}(z) \right)_+ \mid \|z\|_\infty = a, \|z + \delta^*\|_\infty = a + r \right] \\ &= \int \left(\lambda - \left(\frac{1}{1 + \frac{r}{a}} \right)^k e^{-\frac{d-1-k}{2C^2}(2\frac{a}{r}+1)} \right)_+ \pi(a) da \\ &= \int \left(\lambda - \left(1 + \frac{r}{a} \right)^{-k} \left(e^{\frac{2a/r+1}{2C^2}} \right)^{-(d-1-k)} \right)_+ \pi(a) da \\ &= \lambda - \mathcal{O}(t^{-d}),\end{aligned}$$

for some $t > 1$. Here the last equality is by the assumption that $\|z\|_\infty = \mathcal{O}_p(1)$.

Next we bound the second term $\mathbb{E}_a \mathbb{E}_{z \sim \pi_0} \left[\left(\lambda - \frac{\pi_\delta}{\pi_0}(z) \right)_+ \mid \|z\|_\infty = a, \|z + \delta^*\|_\infty \neq a + r \right]$. By the property of uniform distribution, we have

$$\begin{aligned}&\mathbb{P} \left(\frac{|z|^{(d-1)}}{|z|^{(d)}} > (1 - \epsilon) \mid \|z\|_\infty = a, \|z + \delta^*\|_\infty \neq a + r \right) \\ &= \mathbb{P} \left(\frac{|z|^{(d-1)}}{|z|^{(d)}} > (1 - \epsilon) \mid \|z\|_\infty = a \right) \\ &\geq 1 - (1 - \epsilon)^{d-1}.\end{aligned}$$

And thus, for any $\epsilon \in [0, 1)$,

$$\mathbb{P} \left(\|z + \delta^*\|_\infty \geq ((1 - \epsilon)a + r)^2 \mid \|z\|_\infty = a, \|z + \delta^*\|_\infty \neq a + r \right) \geq \frac{1}{2} (1 - (1 - \epsilon)^{d-1}).$$

It implies that

$$\begin{aligned}&\mathbb{E}_{z \sim \pi_0} \left[\left(\lambda - \frac{\pi_\delta}{\pi_0}(z) \right)_+ \mid \|z\|_\infty = a, \|z + \delta^*\|_\infty = a + r \right] \\ &\geq \frac{1}{2} (1 - (1 - \epsilon)^{d-1}) \left(\lambda - \left(1 - \epsilon + \frac{r}{a} \right)^{-k} e^{-\frac{1}{2\sigma^2}(\epsilon(\epsilon-2)a^2 + 2r(1-\epsilon)a + r^2)} \right)_+ \\ &= \frac{1}{2} (1 - (1 - \epsilon)^{d-1}) \left(\lambda - \left(1 - \epsilon + \frac{r}{a} \right)^{-k} e^{-\frac{d-1-k}{2C^2}(\epsilon(\epsilon-2)a^2/r^2 + 2(1-\epsilon)a/r + 1)} \right)_+.\end{aligned}$$

For any $\epsilon' \in (0, 1)$, by choosing $\epsilon = \frac{\log(2/\epsilon')}{d-1}$, for large enough d , we have

$$\begin{aligned}
 & \mathbb{E}_{\mathbf{z} \sim \pi_0} \left[\left(\lambda - \frac{\pi_{\delta}(\mathbf{z})}{\pi_0} \right)_+ \mid \|\mathbf{z}\|_{\infty} = a, \|\mathbf{z} + \delta^*\|_{\infty} = a + r \right] \\
 & \geq \frac{1}{2} \left(1 - (1 - \epsilon)^{d-1} \right) \left(\lambda - \left(1 - \epsilon + \frac{r}{a} \right)^{-k} e^{-\frac{d-1-k}{2C^2} (2(1-\epsilon)a/r+1)} e^{\frac{a^2 \log(2/\epsilon')}{C^2 r^2}} \right)_+ \\
 & = \frac{1}{2} \left(1 - \left(1 - \frac{\log(2/\epsilon')}{d-1} \right)^{d-1} \right) \left(\lambda - \left(1 - \frac{\log(2/\epsilon')}{d-1} + \frac{r}{a} \right)^{-k} e^{-\frac{d-1-k}{2C^2} (2(1-\epsilon)a/r+1)} e^{\frac{a^2 \log(2/\epsilon')}{C^2 r^2}} \right)_+ \\
 & \geq \frac{1}{2} (1 - \epsilon') \left(\lambda - \left(1 - \epsilon + \frac{r}{a} \right)^{-k} e^{-\frac{d-1-k}{2C^2} (2(1-\epsilon)a/r+1)} e^{\frac{a^2 \log(2/\epsilon')}{C^2 r^2}} \right)_+.
 \end{aligned}$$

Thus we have

$$\begin{aligned}
 & \frac{1}{2} \mathbb{E}_a \mathbb{E}_{\mathbf{z} \sim \pi_0} \left[\left(\lambda - \frac{\pi_{\delta}(\mathbf{z})}{\pi_0} \right)_+ \mid \|\mathbf{z}\|_{\infty} = a, \|\mathbf{z} + \delta^*\|_{\infty} \neq a + r \right] \\
 & = \frac{1}{2} (1 - \epsilon') (\lambda - \mathcal{O}(t^{-d})).
 \end{aligned}$$

Combine the bounds, for large d , we have

$$\mathbb{D}_{\mathcal{F}_{[0,1]}}(\lambda \pi_0 \parallel \pi_{\delta^*}) = (1 - \epsilon') (\lambda - \mathcal{O}(t^{-d})).$$

□

B. Practical Algorithm

In this section, we give our algorithm for certification. Our target is to give a high probability bound for the solution of

$$\mathcal{L}_{\pi_0}(\mathcal{F}_{[0,1]}, \mathcal{B}_{\ell_{\infty}, r}) = \max_{\lambda \geq 0} \{ \lambda f_{\pi_0}^{\#} - \mathbb{D}_{\mathcal{F}_{[0,1]}}(\lambda \pi_0 \parallel \pi_{\delta}) \}$$

given some classifier $f^{\#}$. Following [Cohen et al. \(2019\)](#), the given classifier here has a binary output $\{0, 1\}$. Computing the above quantity requires us to evaluate both $f_{\pi_0}^{\#}$ and $\mathbb{D}_{\mathcal{F}_{[0,1]}}(\lambda \pi_0 \parallel \pi_{\delta})$. A lower bound \hat{p}_0 of the former term is obtained through binominal test as [Cohen et al. \(2019\)](#) do, while the second term can be estimated with arbitrary accuracy using Monte Carlo samples. We perform grid search to optimize λ and given λ , we draw N i.i.d. samples from the proposed smoothing distribution π_0 to estimate $\lambda f_{\pi_0}^{\#} - \mathbb{D}_{\mathcal{F}_{[0,1]}}(\lambda \pi_0 \parallel \pi_{\delta})$. This can be achieved by the following importance sampling manner:

$$\begin{aligned}
 & \lambda f_{\pi_0}^{\#} - \mathbb{D}_{\mathcal{F}_{[0,1]}}(\lambda \pi_0 \parallel \pi_{\delta}) \\
 & \geq \lambda \hat{p}_0 - \int \left(\lambda - \frac{\pi_{\delta}(\mathbf{z})}{\pi_0} \right)_+ \pi_0(\mathbf{z}) d\mathbf{z} \\
 & \geq \lambda \hat{p}_0 - \frac{1}{N} \sum_{i=1}^N \left(\lambda - \frac{\pi_{\delta}(\mathbf{z}_i)}{\pi_0} \right)_+ - \epsilon.
 \end{aligned}$$

And we use reject sampling to obtain samples from π_0 . Notice that, we restrict the search space of λ to a finite compact set so the importance samples is bounded. Since the Monte Carlo estimation is not exact with an error ϵ , we give a high probability concentration lower bound of the estimator. Algorithm 1 summarized our algorithm.

Algorithm 1 Certification algorithm

Input: input image x_0 ; original classifier: f^\sharp ; smoothing distribution π_0 ; radius r ; search interval $[\lambda_{\text{start}}, \lambda_{\text{end}}]$ of λ ; search precision h for optimizing λ ; number of samples N_1 for testing p_0 ; pre-defined error threshold ϵ ; significant level α ;

compute search space for λ : $\Lambda = \text{range}(\lambda_{\text{start}}, \lambda_{\text{end}}, h)$

compute N_2 : number of Monte Carlo estimation given ϵ, α and Λ

compute optimal disturb: δ depends on specific setting

for λ **in** Λ **do**

sample $z_1, \dots, z_{N_1} \sim \pi_0$

compute $n_1 = \frac{1}{N_1} \sum_{i=1}^{N_1} f^\sharp(x_0 + z_i)$

compute $\hat{p}_0 = \text{LowerConfBound}(n_1, N_1, 1 - \alpha)$

sample $z_1, \dots, z_{N_2} \sim \pi_0$

compute $\hat{\mathbb{D}}_{\mathcal{F}_{[0,1]}}(\lambda \pi_0 \parallel \pi_\delta) = \frac{1}{N_2} \sum_{i=1}^{N_2} \left(\lambda - \frac{\pi_\delta(z_i)}{\pi_0(z_i)} \right)_+$

compute confidence lower bound $b_\lambda = \lambda \hat{p}_0 - \hat{\mathbb{D}}_{\mathcal{F}_{[0,1]}}(\lambda \pi_0 \parallel \pi_\delta) - \epsilon$

end

if $\max_{\lambda \in \Lambda} b_\lambda \geq 1/2$ **then**

x_0 can be certified

else

x_0 cannot be certified

end

The LowerConfBound function performs a binominal test as described in [Cohen et al. \(2019\)](#). The ϵ in Algorithm 1 is given by concentration inequality.

Theorem 7. Let $h(z_1, \dots, z_N) = \frac{1}{N} \sum_{i=1}^N \left(\lambda - \frac{\pi_\delta(z_i)}{\pi_0(z_i)} \right)_+$, we yield

$$\Pr\{|h(z_1, \dots, z_N) - \int (\lambda \pi_0(z) - \pi_\delta(z))_+ dz| \geq \epsilon\} \leq \exp\left(\frac{-2N\epsilon^2}{\lambda^2}\right).$$

Proof. Given *McDiarmid's Inequality*, which says

$$\sup_{x_1, x_2, \dots, x_n, \hat{x}_i} |h(x_1, x_2, \dots, x_n) - h(x_1, x_2, \dots, x_{i-1}, \hat{x}_i, x_{i+1}, \dots, x_n)| \leq c_i \quad \text{for } 1 \leq i \leq n,$$

we have $c_i = \frac{\lambda}{N}$, and then obtain

$$\Pr\{|h(z_1, \dots, z_N) - \int (\lambda \pi_0(z) - \pi_\delta(z))_+ dz| \geq \epsilon\} \leq \exp\left(\frac{-2N\epsilon^2}{\lambda^2}\right).$$

□

The above theorem tells us that, once ϵ, λ, N is given, we can yield a bound with high-probability $1 - \alpha$. One can also get N when $\epsilon, \lambda, \alpha$ is provided. Note that this is the same as the Hoeffding bound mentioned in Section 4.2 as McDiarmid bound is a generalization of Hoeffding bound.

However, in practice we can use a small trick as below to certify with much less computation:

Algorithm 2 Practical certification algorithm

Input: input image x_0 ; original classifier: f^\sharp ; smoothing distribution π_0 ; radius r ; search interval for λ : $[\lambda_{\text{start}}, \lambda_{\text{end}}]$; search precision h for optimizing λ ; number of Monte Carlo for first estimation: N_1^0, N_2^0 ; number of samples N_1 for a second test of p_0 ; pre-defined error threshold ϵ ; significant level α ; optimal perturbation δ ($\delta = [r, 0, \dots, 0]^\top$ for ℓ_2 attacking and $\delta = [r, \dots, r]^\top$ for ℓ_∞ attacking).

for λ **in** Λ **do**

- sample $z_1, \dots, z_{N_1^0} \sim \pi_0$
- compute $n_1^0 = \frac{1}{N_1^0} \sum_{i=1}^{N_1^0} f^\sharp(x_0 + z_i)$
- compute $\hat{p}_0 = \text{LowerConfBound}(n_1^0, N_1^0, 1 - \alpha)$
- sample $z_1, \dots, z_{N_2^0} \sim \pi_0$
- compute $\hat{\mathbb{D}}_{\mathcal{F}_{[0,1]}}(\lambda \pi_0 \parallel \pi_\delta) = \frac{1}{N_2^0} \sum_{i=1}^{N_2^0} \left(\lambda - \frac{\pi_\delta}{\pi_0}(z_i) \right)_+$
- compute confidence lower bound $b_\lambda = \lambda \hat{p}_0 - \hat{\mathbb{D}}_{\mathcal{F}_{[0,1]}}(\lambda \pi_0 \parallel \pi_\delta)$

end

compute $\hat{\lambda} = \arg \max_{\lambda \in \Lambda} b_\lambda$

compute N_2 : number of Monte Carlo estimation given ϵ, α and $\hat{\lambda}$

sample $z_1, \dots, z_{N_1} \sim \pi_0$

compute $n_1 = \frac{1}{N_1} \sum_{i=1}^{N_1} f^\sharp(x_0 + z_i)$

compute $\hat{p}_0 = \text{LowerConfBound}(n_1, N_1, 1 - \alpha)$

sample $z_1, \dots, z_{N_2} \sim \pi_0$

compute $\hat{\mathbb{D}}_{\mathcal{F}_{[0,1]}}(\lambda \pi_0 \parallel \pi_\delta) = \frac{1}{N_2} \sum_{i=1}^{N_2} \left(\lambda - \frac{\pi_\delta}{\pi_0}(z_i) \right)_+$

compute $b = \hat{\lambda} \hat{p}_0 - \hat{\mathbb{D}}_{\mathcal{F}_{[0,1]}}(\lambda \pi_0 \parallel \pi_\delta) - \epsilon$

if $b \geq 1/2$ **then**

- | x_0 can be certified

else

- | x_0 cannot be certified

end

Algorithm 2 allow one to begin with small N_1^0, N_2^0 to obtain the first estimation and choose a $\hat{\lambda}$. Then a rigorous lower bound can be achieved with $\hat{\lambda}$ with enough (i.e. N_1, N_2) Monte Carlo samples.

B.1. Experiment Settings

The details of our method are shown in the supplementary material. Since our method requires Monte Carlo approximation, we draw $0.1M$ samples from π_0 and construct $\alpha = 99.9\%$ confidence lower bounds of that in Equation (9). The optimization on λ is solved using grid search. For ℓ_2 attacks, we set $k = 500$ for CIFAR-10 and $k = 50000$ for ImageNet in our non-Gaussian smoothing distribution Equation (10). If the used model was trained with a Gaussian perturbation noise of $\mathcal{N}(0, \sigma_0^2)$, then the σ parameter of our smoothing distribution is set to be $\sqrt{(d-1)/(d-1-k)}\sigma_0$, such that the expectation of the norm $\|z\|_2$ under our non-Gaussian distribution Equation (10) matches with the norm of $\mathcal{N}(0, \sigma_0^2)$. For ℓ_1 situation, we keep the same rule for hyperparameter selection as ℓ_2 case, in order to make the norm of proposed distribution has the same mean with original distribution. The certification results of baseline might be slightly different from [Teng et al. \(2020\)](#) in which the whole dataset is assessed while we follow [Cohen et al. \(2019\)](#) to certify a subset with 500 data points. For ℓ_∞ situation, we set $k = 250$ and σ also equals to $\sqrt{(d-1)/(d-1-k)}\sigma_0$ for the mixed norm smoothing distribution Equation (13). More ablation study about k is deferred to Appendix C.

C. Abalation Study

On CIFAR10, we also do ablation study to show the influence of different k for the ℓ_2 certification case as shown in Table 6.

ℓ_2 Radius	0.25	0.5	0.75	1.0	1.25	1.5	1.75	2.0	2.25
Baseline (%)	60	43	34	23	17	14	12	10	8
$k = 100$ (%)	60	43	34	23	18	15	12	10	8
$k = 200$ (%)	60	44	36	24	18	15	13	10	8
$k = 500$ (%)	61	46	37	25	19	16	14	11	9
$k = 1000$ (%)	59	44	36	25	19	16	14	11	9
$k = 2000$ (%)	56	41	35	24	19	16	15	12	9

Table 6. Certified top-1 accuracy of the best classifiers on cifar10 at various ℓ_2 radius. We use the same model as Cohen et al. (2019) and do not train any new models.

D. Illumination about Bilateral Condition²

The results in the main context is obtained under binary classification setting. Here we show it has a natural generalization to multi-class classification setting. Suppose the given classifier f^\sharp classifies an input \mathbf{x}_0 correctly to class A, i.e.,

$$f_A^\sharp(\mathbf{x}_0) > \max_{B \neq A} f_B^\sharp(\mathbf{x}_0) \quad (14)$$

where $f_B^\sharp(\mathbf{x}_0)$ denotes the prediction confidence of any class B different from ground truth label A . Notice that $f_A^\sharp(\mathbf{x}_0) + \sum_{B \neq A} f_B^\sharp(\mathbf{x}_0) = 1$, so the necessary and sufficient condition for correct binary classification $f_A^\sharp(\mathbf{x}_0) > 1/2$ becomes a *sufficient* condition for multi-class prediction.

Similarly, the necessary and sufficient condition for correct classification of the *smoothed* classifier is

$$\min_{f \in \mathcal{F}} \left\{ \mathbb{E}_{\mathbf{z} \sim \pi_0} [f_A(\mathbf{x}_0 + \boldsymbol{\delta} + \mathbf{z})] \quad \text{s.t.} \quad \mathbb{E}_{\pi_0} [f_A(\mathbf{x}_0)] = f_{\pi_0, A}^\sharp(\mathbf{x}_0) \right\} > \max_{f \in \mathcal{F}} \left\{ \mathbb{E}_{\mathbf{z} \sim \pi_0} [f_B(\mathbf{x}_0 + \boldsymbol{\delta} + \mathbf{z})] \quad \text{s.t.} \quad \mathbb{E}_{\pi_0} [f_B(\mathbf{x}_0)] = f_{\pi_0, B}^\sharp(\mathbf{x}_0) \right\}$$

for $\forall B \neq A$ and any perturbation $\boldsymbol{\delta} \in \mathcal{B}$. Writing out their Langragian forms makes things clear:

$$\max_{\lambda} \lambda f_{\pi_0, A}^\sharp(\mathbf{x}_0) - \mathbb{D}_{\mathcal{F}_{[0,1]}}(\lambda \pi_0 \parallel \pi_{\boldsymbol{\delta}}) > \min_{\lambda} \max_{B \neq A} \lambda f_{\pi_0, B}^\sharp(\mathbf{x}_0) + \mathbb{D}_{\mathcal{F}_{[0,1]}}(\pi_{\boldsymbol{\delta}} \parallel \lambda \pi_0)$$

Thus the overall necessary and sufficient condition is

$$\min_{\boldsymbol{\delta} \in \mathcal{B}} \left\{ \max_{\lambda} \left(\lambda f_{\pi_0, A}^\sharp(\mathbf{x}_0) - \mathbb{D}_{\mathcal{F}_{[0,1]}}(\lambda \pi_0 \parallel \pi_{\boldsymbol{\delta}}) \right) - \max_{B \neq A} \min_{\lambda} \left(\lambda f_{\pi_0, B}^\sharp(\mathbf{x}_0) + \mathbb{D}_{\mathcal{F}_{[0,1]}}(\pi_{\boldsymbol{\delta}} \parallel \lambda \pi_0) \right) \right\} > 0$$

Optimizing this *bilateral* object will *theoretically* give a *better certification result* than our method in main context, especially when the number of classes is large. But we do not use this bilateral formulation as reasons stated below.

When both π_0 and $\pi_{\boldsymbol{\delta}}$ are gaussian, which is Cohen et al. (2019)’s setting, this condition is equivalent to:

$$\begin{aligned} & \min_{\boldsymbol{\delta} \in \mathcal{B}} \left\{ \Phi \left(\Phi^{-1}(f_{\pi_0, A}^\sharp(\mathbf{x}_0)) - \frac{\|\boldsymbol{\delta}\|_2}{\sigma} \right) - \max_{B \neq A} \Phi \left(\Phi^{-1}(f_{\pi_0, B}^\sharp(\mathbf{x}_0)) + \frac{\|\boldsymbol{\delta}\|_2}{\sigma} \right) \right\} > 0 \\ \Leftrightarrow & \quad \Phi^{-1}(f_{\pi_0, A}^\sharp(\mathbf{x}_0)) - \frac{r}{\sigma} > \Phi^{-1}(f_{\pi_0, B}^\sharp(\mathbf{x}_0)) + \frac{r}{\sigma}, \quad \forall B \neq A \\ \Leftrightarrow & \quad r < \frac{\sigma}{2} \left(\Phi^{-1}(f_{\pi_0, A}^\sharp(\mathbf{x}_0)) - \Phi^{-1}(f_{\pi_0, B}^\sharp(\mathbf{x}_0)) \right), \forall B \neq A \end{aligned}$$

with a similar derivation process like Appendix A.3. This is exactly the same bound in the (restated) theorem 1 of Cohen et al. (2019).

Cohen et al. (2019) use $1 - p_A$ as a naive estimate of the upper bound of $f_{\pi_0, B}^\sharp(\mathbf{x}_0)$, where p_A is a lower bound of $f_{\pi_0, A}^\sharp(\mathbf{x}_0)$. This leads the confidence bound decay to the bound one can get in binary case, i.e., $r \leq \sigma \Phi^{-1}(f_{\pi_0, A}^\sharp(\mathbf{x}_0))$.

As the two important baselines (Cohen et al., 2019; Salman et al., 2019) do not take the bilateral form, we also do not use this form in experiments for fairness.

²In fact, the theoretical part of Jia et al. (2020) share some similar discussion with this section.